FINAL REPORT ON AEROSOL PRETREATMENT TECHNOLOGY PERFORMANCE AND BENCHMARKING

May 31, 2021

Contributing authors:
Devin Bostick, Linde Gas North America LLC
David Dhanraj, Washington University in St. Louis
Ruan Renhui, Washington University in St. Louis
Benjamin Kumfer, Washington University in St. Louis
Pratim Biswas, Washington University in St. Louis
Wyatt Sherlock, University of Illinois Urbana-Champaign
Christopher Lehmann, University of Illinois Urbana-Champaign
Ravi Jain, InnoSepra LLC
Norberto Lemcoff, InnoSepra LLC

WORK PERFORMED UNDER AGREEMENT
DE-FE0031592

FLUE GAS AEROSOL PRETREATMENT TO MINIMIZE PCC SOLVENT LOSSES
AOI [2] – Enabling Technologies to Improve Carbon Capture Systems

SUBMITTED BY
Linde Gas North America LLC
1 Greenwich St. Suite #100
Stewartsville, NJ 08886

PRINCIPAL INVESTIGATOR
Devin Bostick
Phone: 908-447-0003
Email: devin.bostick@linde.com

SUBMITTED TO
U.S. Department of Energy
Office of Fossil Energy
National Energy Technology Laboratory

Table of Contents

Abbreviations:

PCC: Post-combustion CO_2 capture
UIUC: University of Illinois at Urbana-Champaign
ISTC: Illinois Sustainable Technology Center
WUSTL: Washington University in St. Louis
SMPS: Scanning mobility particle sizer
ACS: Affiliated Construction Services
Abbott: Abbott Power Plant
FGD: Flue gas desulfurization
ESP: Electrostatic precipitator
SCA: Specific collection area
COE: Cost of electricity
For the high-velocity water spray pretreatment technology
N1 & N2: water spray nozzle types tested
LPP: large-sized hole perforated plate, MPP: medium-sized hole perforated plate

A. EXECUTIVE SUMMARY

Solvent-based post-combustion CO_2 capture (PCC) technology remains one of the leading methods to combat global CO_2 emissions produced from large-scale coal-fired power production. Advanced solvent-based PCC technology has made significant improvements in design and performance that reduce capital and operating costs to enable its commercial use. Key to low cost, manageable logistics, and environmentally safe operation of solvent-based PCC technology are minimal solvent losses from the process through the treated gas stream exiting PCC plant absorbers. High flue gas aerosol particle concentrations (>10^5 particles/cm^3) for particles in the range of 70-200 nm have been shown to cause significant amine solvent losses for solvent-based PCC processes through several mechanisms including absorption of solvent and water into growing aerosol particles. Flue gas aerosol pretreatment technology is the only realistic and economically attractive method to reduce very high aerosol particle concentrations (>10^7 particles/cm^3) to enable solvent-based PCC for existing power plants lacking sufficient particle removal systems, such as baghouses.

The overall goal of this project was to design, construct, independently test, and evaluate three flue gas aerosol pretreatment technologies identified to significantly reduce high aerosol particle concentrations (>10^7 particles/cm^3) in the 70-200 nm particle size range: (1) a novel, high-velocity water injection spray concept developed by RWE and tested by Linde, (2) an innovative electrostatic precipitator (ESP) device with optimized operating conditions developed by Washington University in St. Louis (WUSTL), and (3) a non-regenerative sorbent-based filter technology developed by InnoSepra for SO_x and NO_x removal from coal-fired power plant flue gas. Each technology has been validated with tests on 500-1000 scfm of actual coal-fired flue gas and evaluated in terms of particle removal efficiency (%), cost competitiveness, and environmental impact. Aerosol measurements were performed upstream and downstream of each aerosol reduction unit during independent testing of each technology using advanced instrumentation and analytical methods provided by WUSTL. To perform aerosol measurements, isokinetic probes were inserted into flanged pipes attached to the flue gas piping, and a small suction pump was used to sample gas containing aerosol particles. Aerosol particle number concentrations (# particles/cm^3) and size distributions were then measured using a scanning mobility particle sizer (SMPS, TSI Inc.) for very fine particles (<1,000 nm) and a particle counter manufactured by GRIMM for particles larger than 1,000 nm. This report summarizes the aerosol removal performance results from pilot scale testing of each technology. Performance results have been benchmarked against pre-defined targets and other flue gas aerosol pretreatment technologies with documented performance. **Linde Gas North America LLC** has been the prime contractor to DOE responsible for overall project management and provided the design for the high-velocity water spray-based aerosol removal technology based on a design concept developed by the German utility company RWE. Other team members include:

WUSTL - responsible for modeling aerosol nucleation & growth mechanisms and designing & building the ESP-based aerosol removal technology

InnoSepra – responsible for providing their non-regenerative sorbent technology

The University of Illinois Urbana-Champaign (UIUC) – Abbott Power Plant host site provider and responsible for performing composition analysis for the flue gas supply & treated gas return streams and liquid condensate analysis for the spray-based system

Affiliated Construction Services (ACS) - responsible for procurement and construction management of the RWE water spray-based system, InnoSepra filter housing, and structural components & interconnecting piping for the pilot skid, including piping for flue gas supply and return, cooling water, and instrument air lines.

Flue gas aerosol characterization measurements at the Abbott host site have revealed very high flue gas aerosol particle concentrations (>10^7 particles/cm^3) for particles in the range of 70-200 nm. The Abbott site therefore provides a unique platform for evaluation of aerosol mitigation technologies over a wide range of aerosol particle concentrations and size distributions expected for commercial power plant flue gas streams. Flue gas aerosol pretreatment technologies that greatly reduce aerosol concentrations will enable integration of solvent-based PCC technology with most existing coal-fired power plants by minimizing solvent losses.

B. TECHNOLOGY BACKGROUND

B.1 Mechanisms for aerosol-driven amine losses and critical importance of aerosol pretreatment

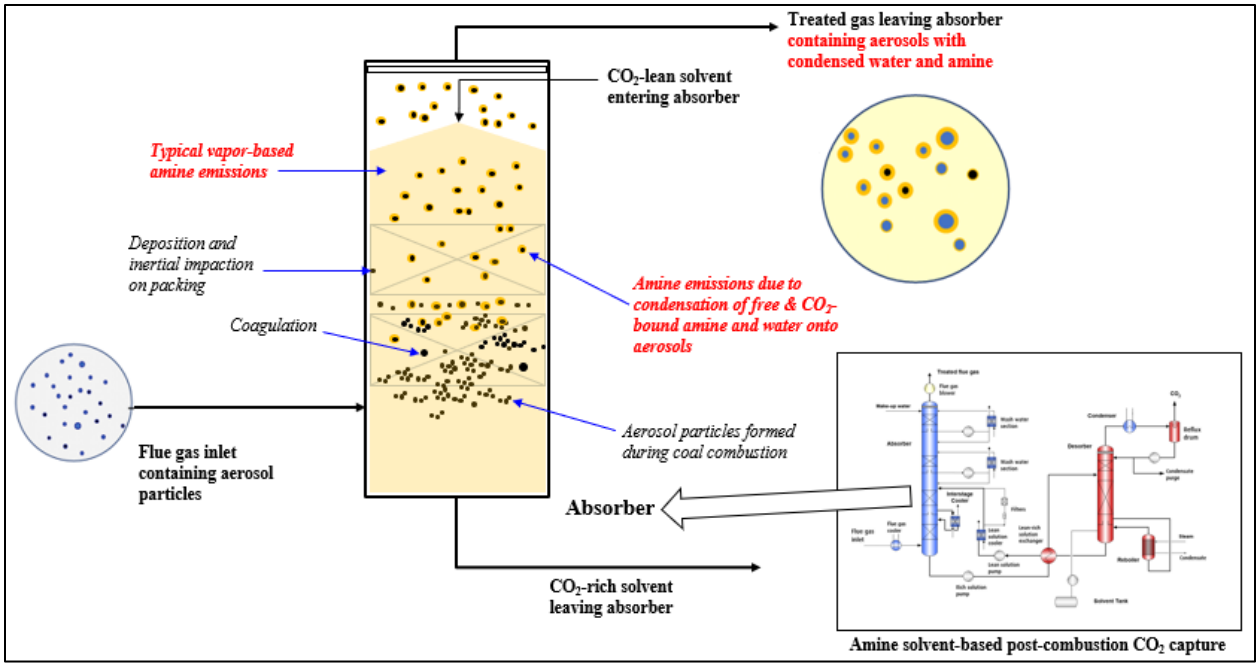

Figure 1: Aerosol-driven amine loss mechanisms summary

Figure 1 illustrates the problem caused by flue gas aerosol particles that carry out solvent from the absorbers of PCC systems. A few likely aerosol-driven solvent loss mechanisms described in scientific literature are based on principles such as the kelvin equation for minimum particle diameter of a liquid, and include (1) aerosol growth from water and homogeneous nucleation from high water supersaturation, (2) aerosol growth from amine until complete amine saturation in the aerosols, (3) buildup of captured CO_2 along with amine bound to the CO_2 inside aerosol particles, and (4) salt accumulation inside aerosol particles enabling amine and CO_2 diffusion into aerosols. Amine emissions are denoted in red text in Figure 1. The initial size of particles, the initial particle density, and the aerosol growth rate due to water condensation and absorption are major contributors to aerosol-driven amine losses. Another critical factor is the difference in temperature between the CO_2-lean solvent and the flue gas, which enables supersaturation of water and amine in the gas phase. Any supersaturation can lead to amine losses even at low aerosol particle densities. Supersaturation becomes a concern above the highest absorption section where relatively cold CO_2-lean solution enters the absorber and cools warm flue gas. The sudden cooling increases the concentrations of condensable components in the gas phase above their vapor-liquid equilibrium concentrations. The gas phase becomes supersaturated with high amine concentrations, and subsequent water condensation creates and enlarges aerosol particles containing amine from the gas phase. These amine-saturated aerosol particles continue to grow and multiply through the wash water sections and demister at the top of the absorber and eventually carry amine out of the absorber with the treated gas. In a typical PCC plant absorber design, water wash sections above the absorption sections at the top of the column are used to recover most of the amines leaving the absorber in the gas phase. The temperature of the top water wash section must be carefully controlled to maintain the water balance of the PCC plant. Of course, changing the operating conditions of the absorber greatly impacts the performance of the solvent and ultimately the specific regeneration energy of the process (MJ/kg CO_2), so any process changes meant to reduce aerosol-driven solvent losses need to be assessed to provide the best overall outcome in terms of cost, safety, and reliability. Even if optimum conditions for the water wash sections are used, when aerosol concentrations are too high to sustain PCC plant normal operation, absorber operating conditions may need to be changed so drastically to reduce solvent losses that the resulting specific energy requirement becomes prohibitively high. In this situation,

alternative methods to reduce aerosol concentrations are needed, and flue gas pretreatment technologies offer the only solution. It has been shown that power plants equipped with a baghouse produce flue gas with far lower aerosol particle concentrations (<10^5 particles/cm^3) compared to those without a baghouse (>10^7 particles/cm^3). Installation and maintenance of a new commercial baghouse at an existing power plant involves significant capital and labor cost as well as a large site footprint, so effective flue gas aerosol pretreatment options immediately upstream of the PCC absorber are in comparison much more economically attractive and feasible to mitigate nano-sized aerosols in particular. Although recently built coal-fired power plants are expected to include baghouses to comply with new particulate matter emission limits, many existing power plants do not have baghouses and would need effective aerosol pretreatment when retrofitted with a PCC plant. Hence, this work has focused on development and evaluation of flue gas aerosol pretreatment options for PCC plants recovering CO_2 from power plants not equipped with baghouses where very high aerosol particle concentrations in the small particle size distribution range (70-200 nm) are expected.

B.2 Aerosol-driven amine loss data and findings from previous PCC pilot plant testing

It has been shown that the extent of aerosol-driven amine losses depends on the range of aerosol particle sizes present in the flue gas upstream of the PCC plant, certain particle sizes impact solvent losses more so than others. Literature studies have shown that high concentrations (>10^5 particles/cm^3) of very fine aerosol particles with particle diameters below 200 nm cause the most severe amine losses because demister systems in direct contact coolers (DCC), scrubbers, and CO_2 absorbers are most effective at capturing particles with diameters above 200 nm along with any entrained amine in the gas phase [Ref. 1]. A common metric used industrially to evaluate solvent losses for PCC plants is the threshold of 0.3 kg amine/tonne CO_2 captured based on published monoethanolamine (MEA) losses for solvent-based PCC processes. Above this metric, solvent makeup rates become less logistically feasible, so it provides a useful benchmark for evaluating the viability of PCC technologies combined with flue gas conditions. Figures 2 and 3 show the impact of aerosol particle concentrations (left plot) on amine losses (right plot) from the absorber before and after installation of a baghouse in 2016, as measured in parametric tests performed at the Linde-BASF 1.5 MWe PCC pilot plant tested at the National Carbon Capture Center (NCCC) [Ref. 2].

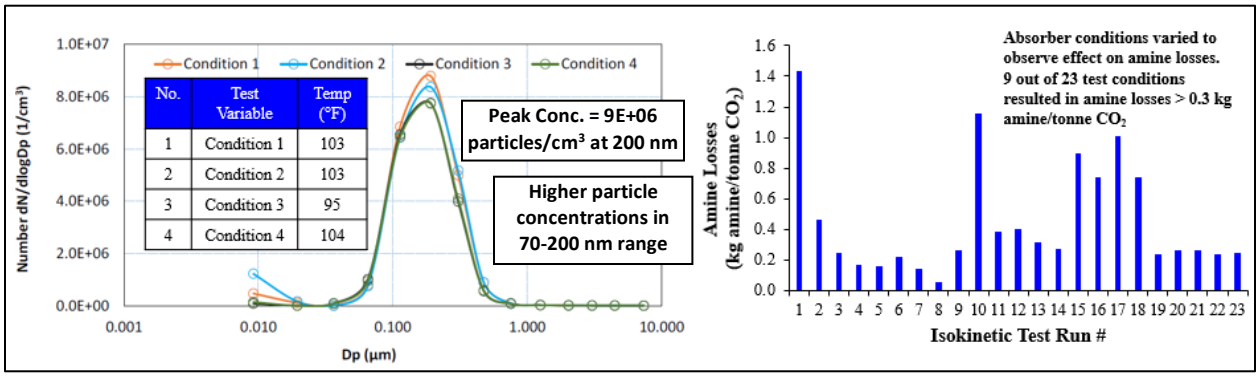

Figure 2: Aerosol and amine loses measurements completed at the Linde-BASF 1.5 MWe PCC pilot from August 2015 to December 2015 before baghouse installation at NCCC

Regardless of the type of aerosol pretreatment (baghouse), lowering the aerosol concentrations leads to significant reductions in amine losses from PCC plants. Notably, the highest particle concentration before the baghouse (9.0E+06 particles/cm^3) at 200 nm particle diameter was reduced to 1.0E+04 particles/cm^3 after the baghouse was installed. As depicted in the lower left plot, the particle concentrations for 20-70 nm particles do not seem to greatly influence solvent losses. Moreover, the data in Figure 2 indicate that high concentrations (>10^5 particles/cm^3) of particles with diameters between 70 nm and 200 nm seem to increase solvent losses most significantly.

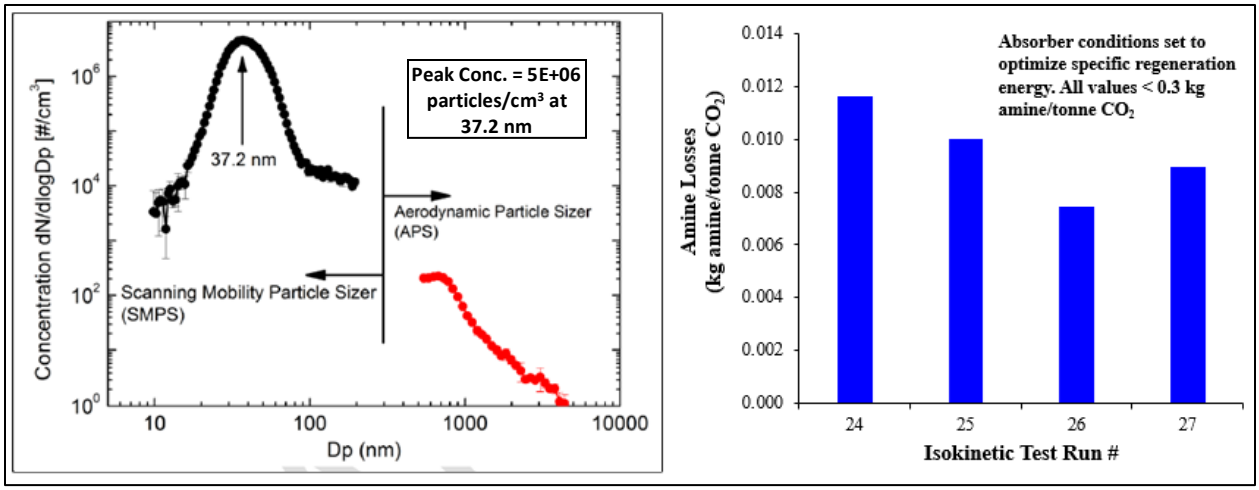

Figure 3: Aerosol and amine loses measurements completed at the Linde-BASF 1.5 MWe PCC on 7/21/16 after baghouse installation at NCCC

The results shown in Figures 2 and 3 are based on testing with BASF's OASE® blue solvent. Similar results can be achieved for other amine-based solvents, such as MEA. Hence, the benefits of reducing aerosol concentrations for certain particle sizes in the 70-200 nm range can be observed for any solvent-based PCC system. Based on results from previous Linde-BASF PCC pilot tests at NCCC, varying the absorber operating conditions for each test condition shown (right plot of Figure 2) to determine a set of conditions that minimized solvent losses negatively affected the specific energy consumption of the Linde-BASF PCC pilot by as much as 20%, rendering such changes potentially cost-prohibitive at large scale.

B.3 Aerosol particle size distribution and number concentration: scientific literature review

Flue gas aerosol particle size and concentration measurements were performed at Abbott WUSTL in February 2016 to evaluate the impact of aerosol particles as part of a Phase I pre-engineering study for a Linde-BASF large PCC pilot submitted under DE-FE0026588.

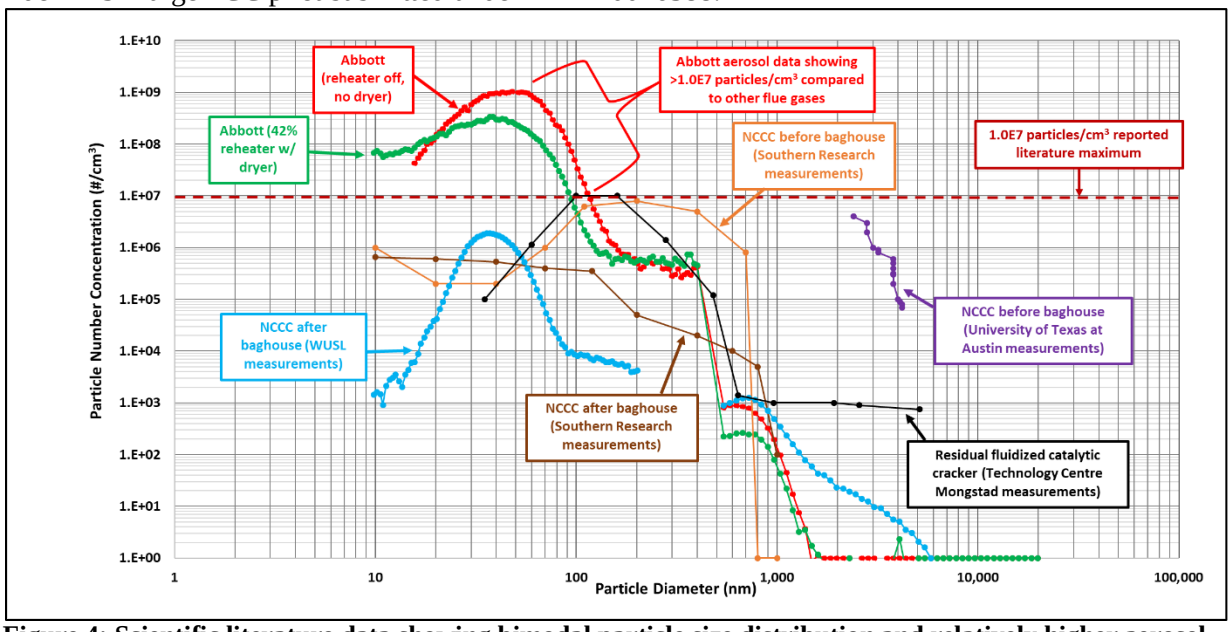

Figure 4: Scientific literature data showing bimodal particle size distribution and relatively higher aerosol particle concentrations for Abbott Power Plant flue gas (>1.0E7 particles/cm^3) for very small particles (<100 nm) compared to other power plant flue gases

A summary of the data collected at Abbott along with several data sets found from scientific literature is shown in Figure 4 [Ref. 3, 4, 5, 7, 8 & 9]. As shown, the flue gas exiting the Abbott stack has aerosol particle concentrations that are significantly higher than a threshold concentration of 10^7 particles/cm^3 found in most literature studies. Most Abbott flue gas aerosol particle concentrations measured are >10^7 particles/cm^3, of which several are close to 10^9 particles/cm^3 for particles less than 200 nm in size. These results indicate that Abbott is an excellent facility for overall evaluation of aerosol reduction technologies.

B.4 Importance of flue gas aerosol pretreatment compared to other aerosol mitigation methods

Aerosol mitigation methods to reduce aerosol-driven amine losses include (1) baghouse installation in the flue gas upstream of the PCC plant, (2) amine wash sections and wash section operating conditions, (3) specific absorber operating conditions that also negatively impact specific regeneration energy, and (4) flue gas aerosol pretreatment, which is the focus of this research. Based on data from Linde-BASF pilot testing at NCCC (Figure 3), a baghouse installed upstream of the PCC absorber can reduce particle concentrations to <10^5 particles/cm^3 for 70-200 nm size particles. For power plants without a baghouse, other aerosol mitigation options will likely be needed if flue gas particle concentrations exceed 10^5 particles/cm^3. For flue gas with aerosol particle concentrations between 10^5 and 10^6 particles/cm^3, studies have shown that specific water wash section operating conditions at the top of the absorber can sufficiently reduce the effect of flue gas aerosol particles on solvent losses and provide an effective long-term operating solution enabling solvent make-up rates significantly below the 0.3 kg amine/tonne CO_2 threshold. In particular, Linde and BASF's patented dry-bed configuration has been shown to reduce solvent losses from the absorber, as illustrated in Figure 4 [Ref. 6] for flue gas with particle concentrations above 10^6 particles/cm^3.

The dry bed configuration can enable manageable solvent make-up rates (significantly less than 0.3 kg amine/tonne CO_2) during PCC plant operation when particle concentrations are maintained between 10^5 and 10^6 particles/cm^3. The data in Figure 5 was collected at a 0.5 MWe PCC pilot an RWE lignite-fired power plant.

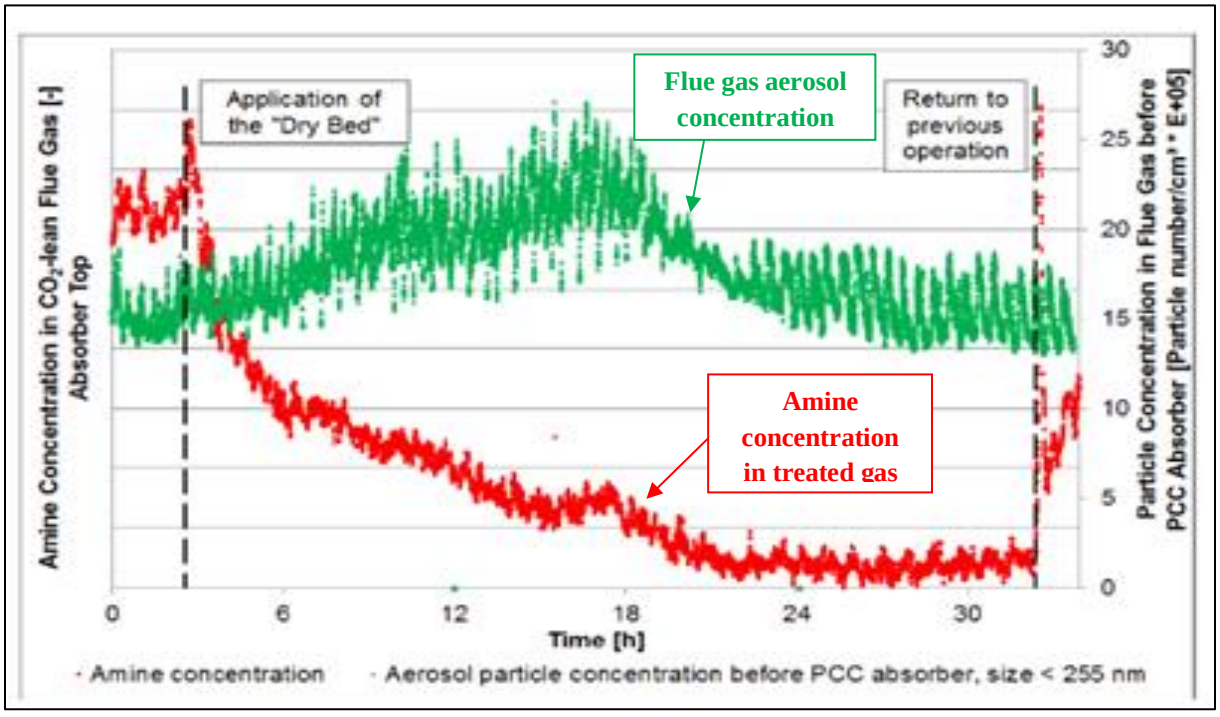

Figure 5: Effect of patented dry bed emission control system on solvent emissions from the absorber column. Amine concentrations are red dots and aerosol particle concentrations are green dots.

For flue gas with particle concentrations between 10^6 and 10^7 particles/cm^3, specific absorber operating conditions can also be used to reduce aerosol-driven amine losses with the treated gas from the absorber. The following process parameters reduced amine losses 5-10 times when combined at the Linde-BASF PCC pilot at NCCC before installation of the baghouse (where particle concentrations exceeded 10^6 particles/cm^3): (1) higher CO_2-lean solution return temperature to the absorber (relative to 104 ºF design temperature), (2) higher temperature of the return solution from the absorption intermediate cooler (relative to 104 ºF design temperature), (3) increased absorber pressure (relative to ~0.99-0.93 bara operating pressure), and (4) reduced treated gas temperature (relative to 43.7 ºC design temperature) [Ref. 10].
As shown in Figure 1, combinations of these parameters achieved solvent loss reduction by altering the size and concentration of aerosol particles at various stages inside the absorber. While effective at reducing aerosol-driven solvent losses, use of the four absorber operating conditions described leads to high specific

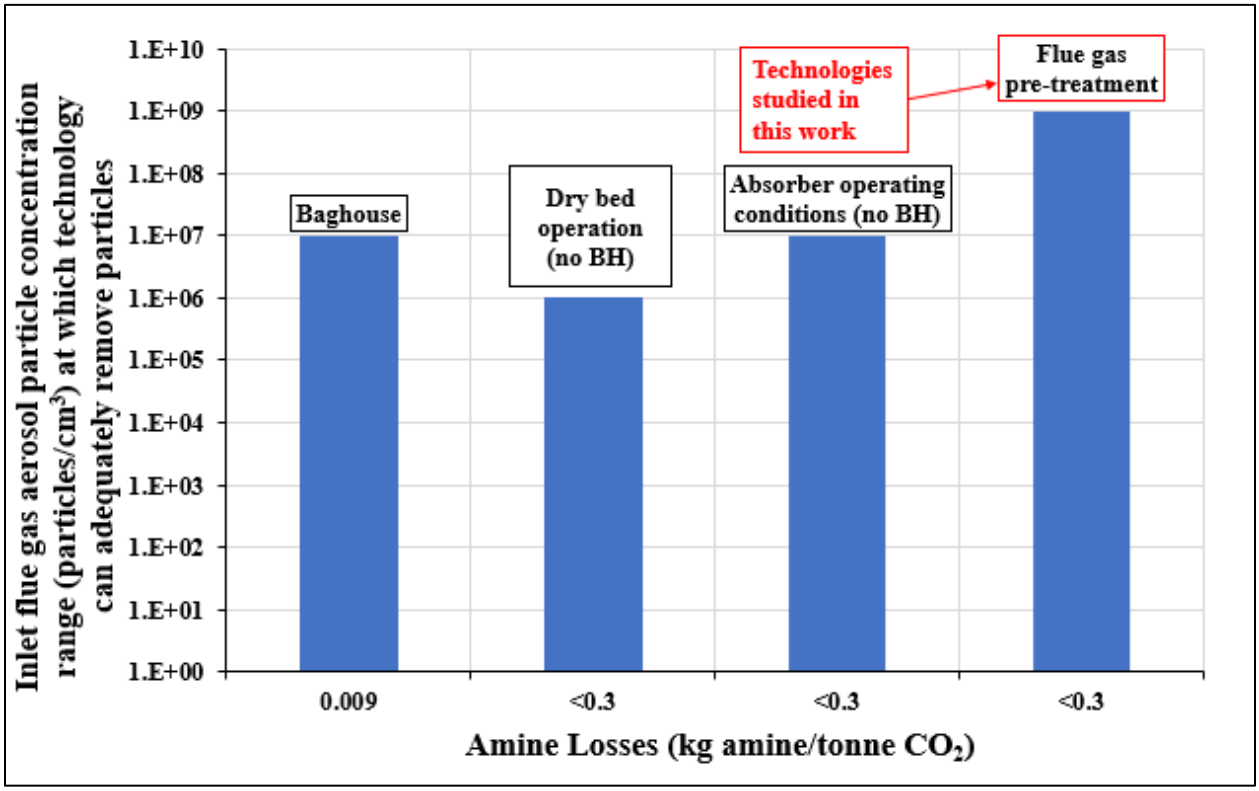

Figure 6: Flue gas aerosol particle concentration ranges for which current technologies are applicable and sufficient

regeneration energies that would make any PCC technology very expensive at commercial scale. Hence, for large-scale PCC processes, varying absorber conditions should only be used as a temporary last resort aerosol mitigation option until a better long-term solution can be implemented. The factors listed above justify the need to improve aerosol reduction capabilities beyond those provided by water wash sections and absorber operating conditions, particularly if flue gas particle concentrations are >10^5/cm^3. Figure 6 shows the range of aerosol particle densities able to be managed by current methods used today to provide <0.3 kg amine/tonne CO_2 solvent losses. For power plants without a baghouse producing flue gas with particle concentrations > 10^7 particles/cm^3, the only realistic option available to mitigate aerosol-driven amine losses from PCC plants is flue gas aerosol pretreatment. Flue gas aerosol pretreatment has traditionally been performed using simple ESPs and Brownian filters, but no systematic study has been performed to evaluate the performance of these systems over the entire range of possible operating conditions, aerosol concentrations, and particle sizes. It is critically important to note that even with lower flue gas aerosol densities (<10^7 particles/cm^3), there is still a sizeable benefit in using pretreatment systems

to minimize amine losses for the entire range of solvent-based PCC operating conditions. Hence, the proposed work focuses on evaluation of flue gas aerosol pretreatment solutions to determine an optimum technology that can minimize aerosol-driven amine losses for any power plant, including plants producing flue gas with the highest range of possible flue gas aerosol concentrations and size distributions.

B.5 Flue gas aerosol pretreatment solutions tested in this work

B.5.1 RWE high-velocity water spray-based system

As shown in Figure 7, the design of RWE's high-velocity water spray-based technology incorporates unique spray nozzle distributors that enable rapid growth and collection of aerosol particles in the liquid phase via water condensation. In addition, the perforated plate at the bottom of the contact vessel optimizes vapor-liquid distribution. Aerosol particles are collected in the liquid-phase process condensate that is continuously discharged during operations and effectively removed from the treated flue gas leaving the top of the vessel. The RWE system built for this project was designed to process up to 1000 scfm flue gas.

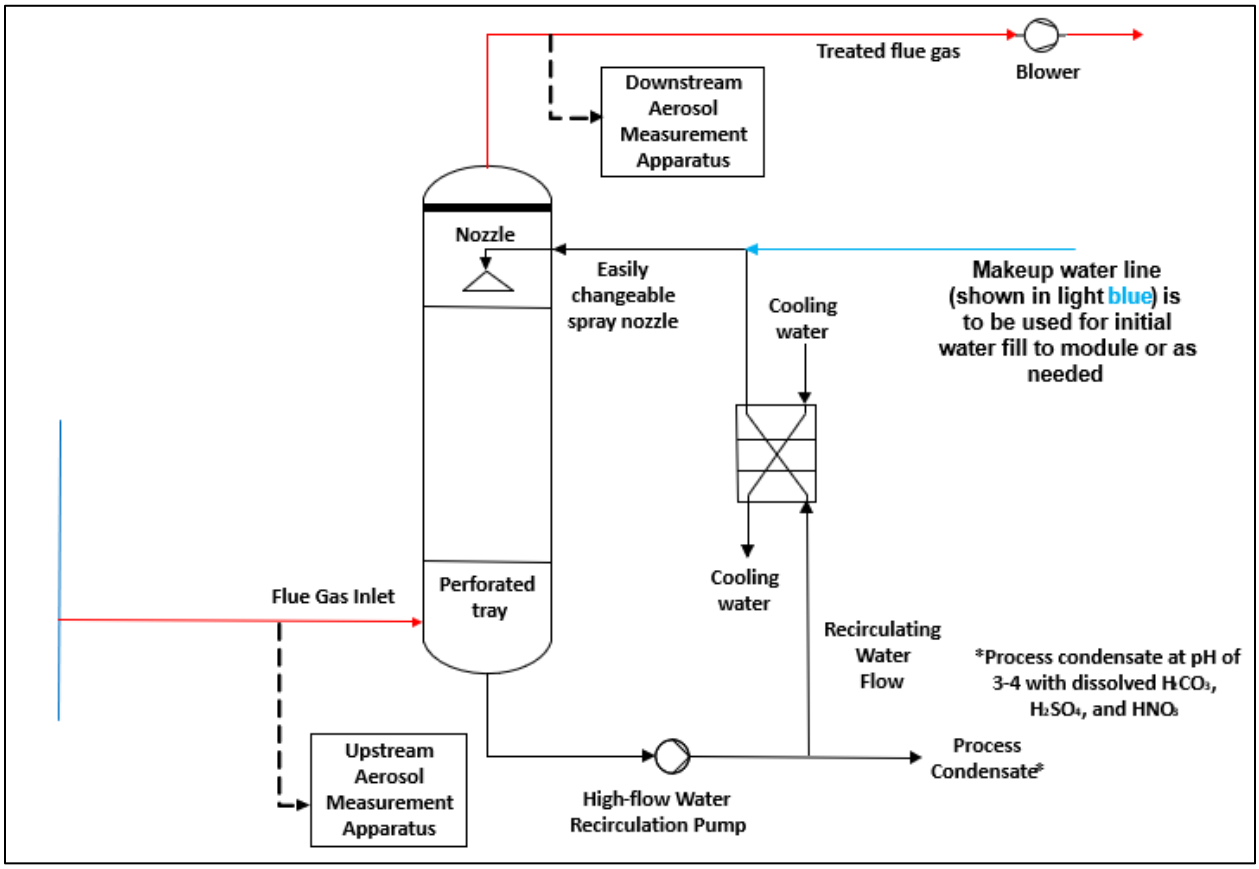

Figure 7: RWE high-velocity water spray-based system

B.5.2 Advanced WUSTL ESP system

A Photoionization Enhanced 2-staged Electrostatic Precipitator (PI-ESP) was designed and fabricated in collaboration with Applied Particle Technology (APT) and a vendor (Laciny Bros.). The two stages are a pre-charging stage and a collection stage. The PI-ESP was designed to treat a volume flow of 500 scfm of flue gas from a coal fired power plant. The entire body was built using stainless steel to handle corrosion. The three stages and the electrical components are enclosed in a weatherproof enclosure. The flow cross sectional area is 22" x 22", with 22 wires in the charging stage (2" depth). The working section is 5.5' tall and the total height including the struts is 8'. The PI-ESP with its different stages is shown in Fig. 8 (left).

The velocity of a particle in the flue gas (at 500 scfm) inside the PI-ESP would be 0.6375 m/s and hence its residence time is 0.08 s in the charging and 0.478 s in the collection stage. The photoionization stage consists of four soft X-ray heads mounted on each of the 4 walls on the stage at a 13-degree angle (see Fig. 8 (right)). The heads irradiate X-rays at 150 degree and hence were spaced at 3" from the plane of the wires such that the coverage at the wires is maximum. Expanded metal (hex mesh) was placed between each wire in the charging stage and in between the X-ray heads and the plane of the wires in the photoionization stage. The X-ray heads, the expanded metal in between the wires, and every alternating plate was grounded while the wires, the expanded metal between the heads the wires (potential grill) and the rest of the plates were applied a positive potential (DC). This design facilitates the generation of unipolar ions in the photoionization stage and the charging stage.

The novel ESP system that has proven its ability to reduce flue gas aerosol concentrations. The ESP works by applying a high voltage between a plate and a wire. This voltage ionizes the aerosol particles in the flue gas. Due to electrostatic force, ionized particles are diverted from the gas towards collecting plates, removing them from the gas. The specific collection area (SCA) of an ESP is the most important design parameter in terms of achieving high aerosol removal efficiencies. A typical SCA for an ESP capable of obtaining 98-99% removal efficiency for 1000 scfm of flue gas flow is ~95 $m^2/(m^3/s)$; this area can be further increased to remove particles in the range of 10-500 nm at very high efficiencies. In this work, the WUSTL ESP system has been tested and validated to remove aerosol particles from flue gas at a capacity of up to 500 scfm. Moreover, WUSTL's incorporated a patented photo-ionizer device upstream of the charging stage that can further enhance aerosol capture efficiency [Ref. 13]. In commercial applications, this photo-ionizer can be retrofitted to existing ESP systems at power plants, further reducing capital costs. A process flow diagram of the lab-scale WUSTL ESP is shown in the left diagram of Figure 8.

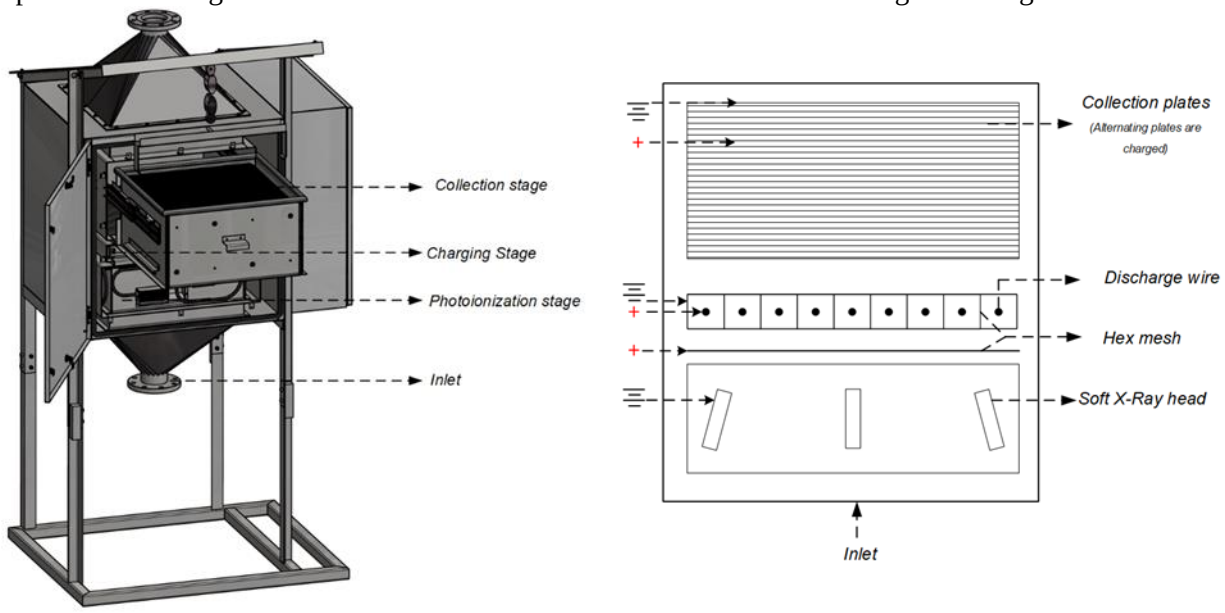

Figure 8: WUSTL ESP system

Specific ESP voltages may increase particle concentrations for certain particle sizes due to secondary aerosol generation inside the ESP from nucleation of H_2O-H_2SO_4 aerosols as SO_2 in the flue gas is oxidized, so the voltage of the ESP needs to be carefully optimized during testing and operations.

B.5.3 InnoSepra sorbent filter for flue gas contaminant removal

InnoSepra has already developed a non-regenerative sorbent technology in a packed bed for flue gas contaminant removal upstream of PCC processes. A process flow diagram of the InnoSepra sorbent filter technology is shown in Figure 9. The sorbent material provides cost-effective removal of residual SO_3, SO_2, NO_2, HCl, and HF from PCC flue gas after flue gas desulfurization (FGD) and offers benefits for aerosol particle reduction, as discussed in this report.

Sorbent material validation tests completed in this work demonstrate:

- >99% SO_2 and SO_3 removal for both impregnated and non-impregnated sorbents
- Very high capacities (20-30 wt%) for feed SO_2 & SO_3 concentrations of 5-15 ppmv
- Low material production costs (<$0.20-0.75/lb)
- Best results can be achieved with impregnated materials
- 30 wt% SO_2 capacity for feeds containing 12-30 ppmv SO_2

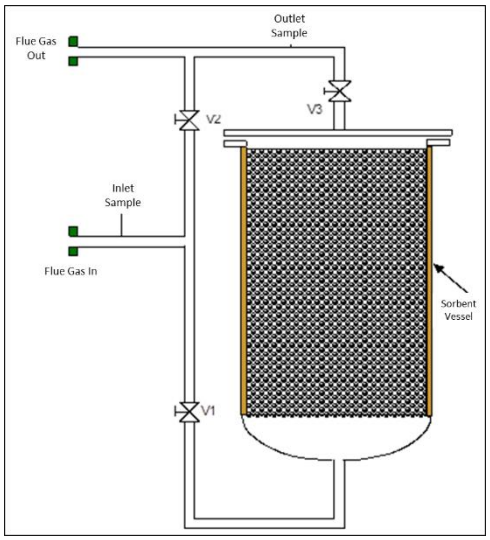

Figure 9: InnoSepra sorbent filter technology

C. FLUE GAS AEROSOL PRETREATMENT PILOT TEST RESULTS

C.1 Pilot plant description and test campaign schedule

The aerosol pretreatment pilot tests were completed at the Abbott host site in Champaign, IL over a period of approximately 8 weeks between 1/2/20 and 3/17/20. A layout of the pilot plant in relation to the utilities and surrounding structures at Abbott and the supply & return flue gas piping connected to the Abbott plant stack is shown in Figure 10.

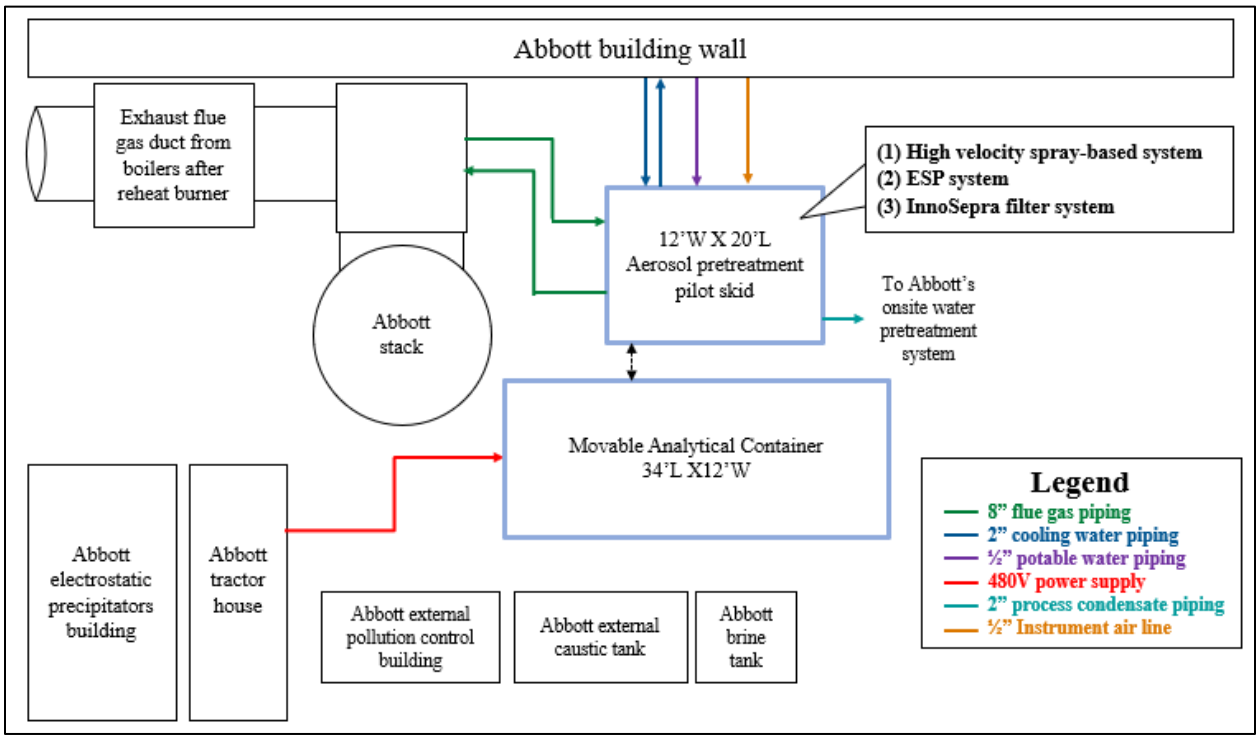

Figure 10: Aerosol pretreatment pilot plant layout in relation to Abbott host site

Pictures of the completed pilot plant construction are shown in Figures 11, 12, 13, and 14. Details of the interconnecting process piping, main programmable logic controller (PLC) cabinet, and other equipment are shown in Figure 15. The pilot skid is composed of the three aerosol pretreatment technologies and designed such that each technology can be independently tested on real coal-fired flue gas from Abbott or tested in series for combination performance. An analytical trailer beside the pilot skid housed the process control screen and operator station as well as analyzer rack for gas composition measurements (CO_2, O_2, SO_2, NO and NO_2). The trailer also contained the aerosol measurement equipment. A Fourier-transform infrared (FTIR) spectroscopy unit was placed outside next to the trailer for additional gas composition measurements. The calibration gas system also housed outside of the trailer.

Testing of the high velocity water spray-based system, ESP, and InnoSepra filter was completed from 1/14/20 to 2/19/20, 1/28/20 to 3/16/20, and 2/19/20 to 3/14/20, respectively. Pilot testing was paused on 2/21/20 and resumed on 3/3/20 after to a 2-week coal boiler shutdown at Abbott for routine maintenance. Pilot testing ended on 3/17/20 when coal-fired operation stopped at Abbott for the spring 2020 season.

Figure 11: Flue gas aerosol pretreatment pilot plant (view facing south east)

Figure 12: Flue gas aerosol pretreatment pilot plant (view facing north west)

Figure 13: Flue gas aerosol pretreatment pilot plant (view facing north)

Figure 14: Flue gas aerosol pretreatment pilot plant (view facing south)

Figure 15: Details of the interconnecting process piping, main programmable logic controller (PLC) cabinet, and other equipment

C.2 Pilot test results

C.2.1 Measurements of aerosol number concentrations and size distributions

Figure 16 shows the apparatus used during pilot tests for particle number concentration and size distribution measurements. The SMPS and GRIMM devices provide the analytical measurements for the fine particle size range of interest.

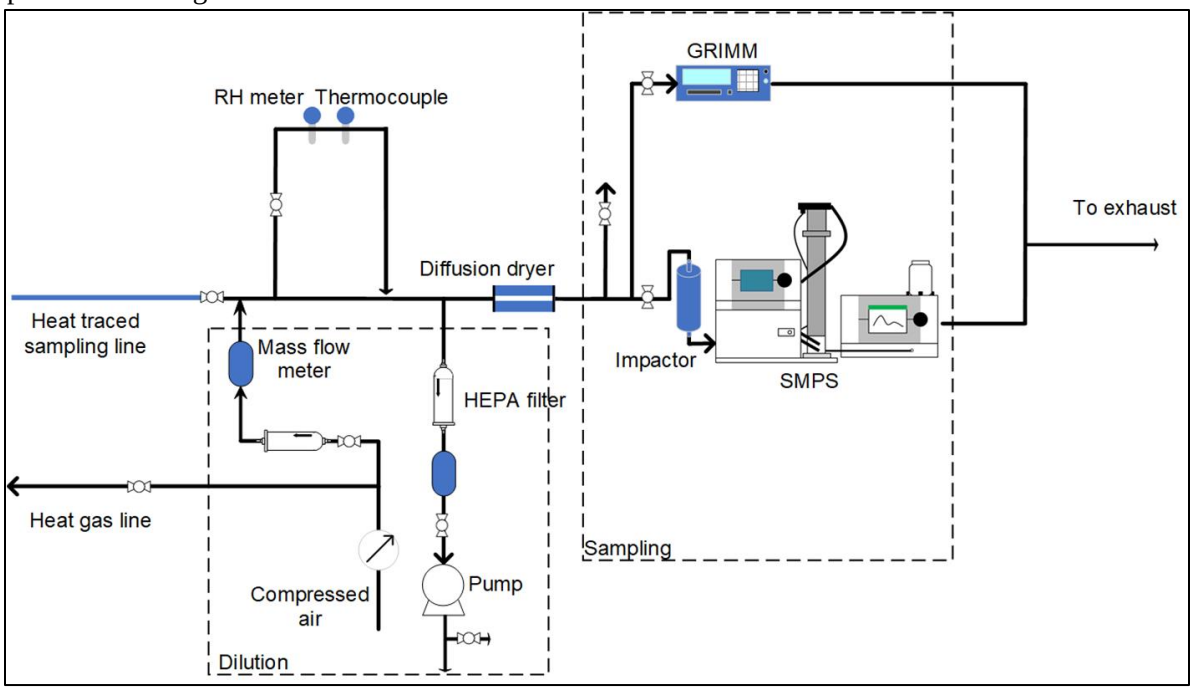

Figure 16: Apparatus used during pilot tests for aerosol particle number concentration and size distribution measurements

Figures 17a-b and 18a-b show typical plots of the flue gas supply aerosol particle number concentration and size distribution measurements during operation of one coal boiler and two coal boilers at Abbott, respectively. Each data set is based on 1000 scfm flue gas flow supplied to the pilot skid.

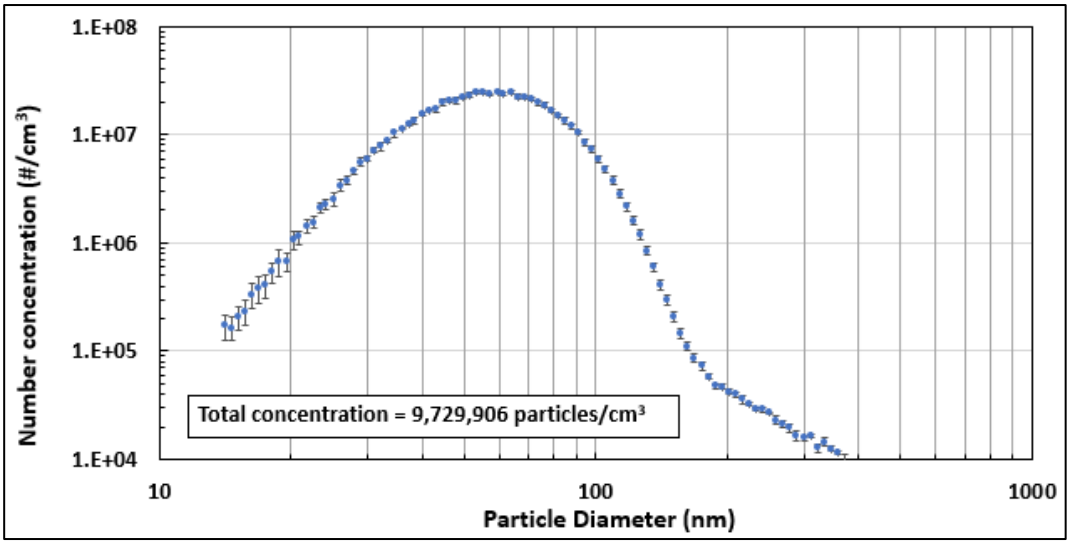

Figure 17a: Average flue gas supply aerosol number concentration and size distribution measurements during operation of one coal boiler (96,000 lb/hr boiler steam rate, date: 1/30/2020, 1,000 scfm flue gas flow)

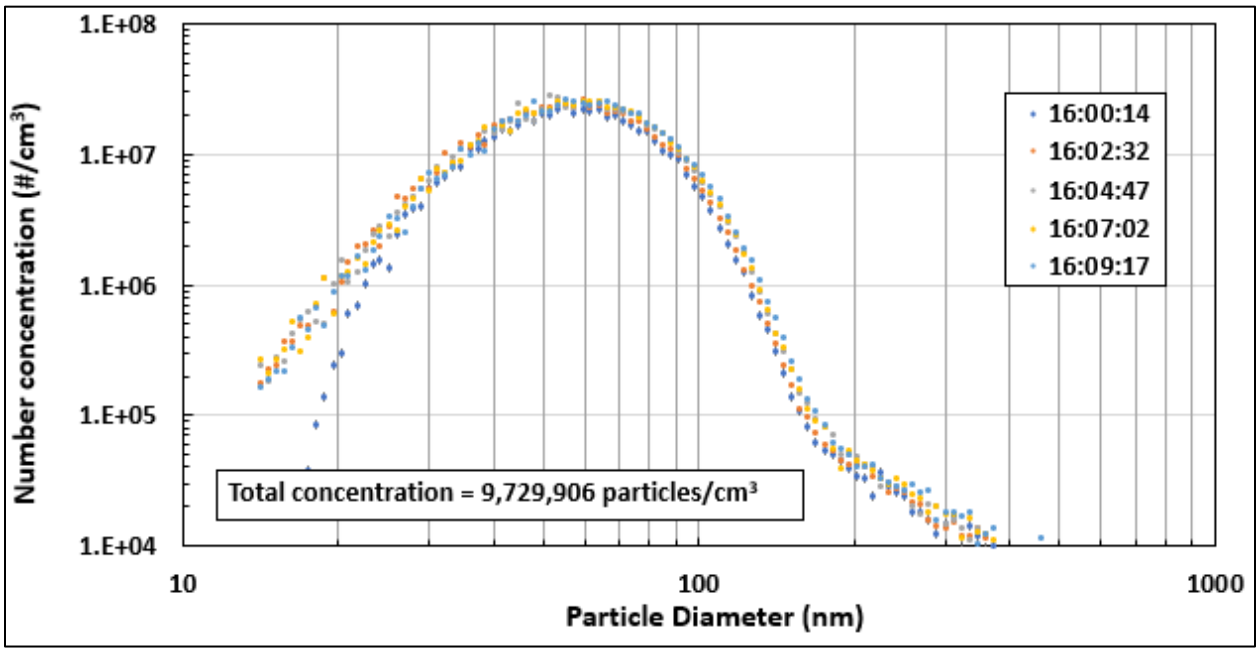

Figure 17b: Flue gas supply aerosol number concentration and size distribution measurements for different samples during operation of one coal boiler (96,000 lb/hr boiler steam rate, date: 1/30/2020, 1,000 scfm flue gas flow)

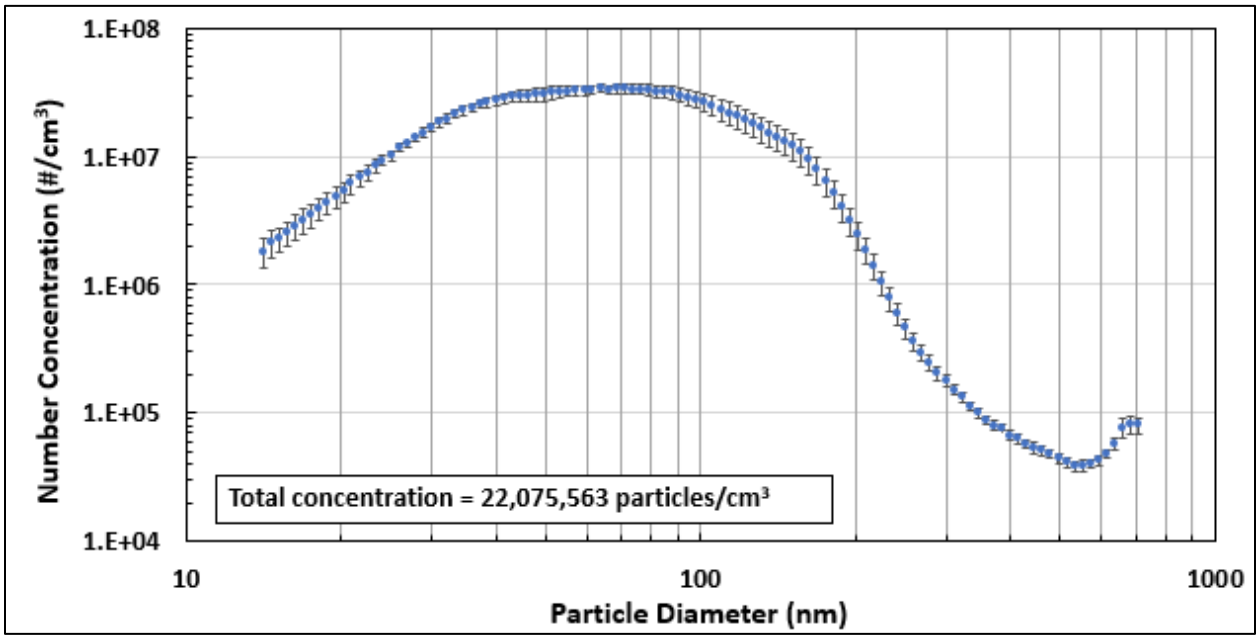

Figure 18a: Average flue gas supply aerosol number concentration and size distribution measurements during operation of two coal boilers (187,000 lb/hr boiler steam rate, date: 2/5/2020, 1,000 scfm flue gas flow)

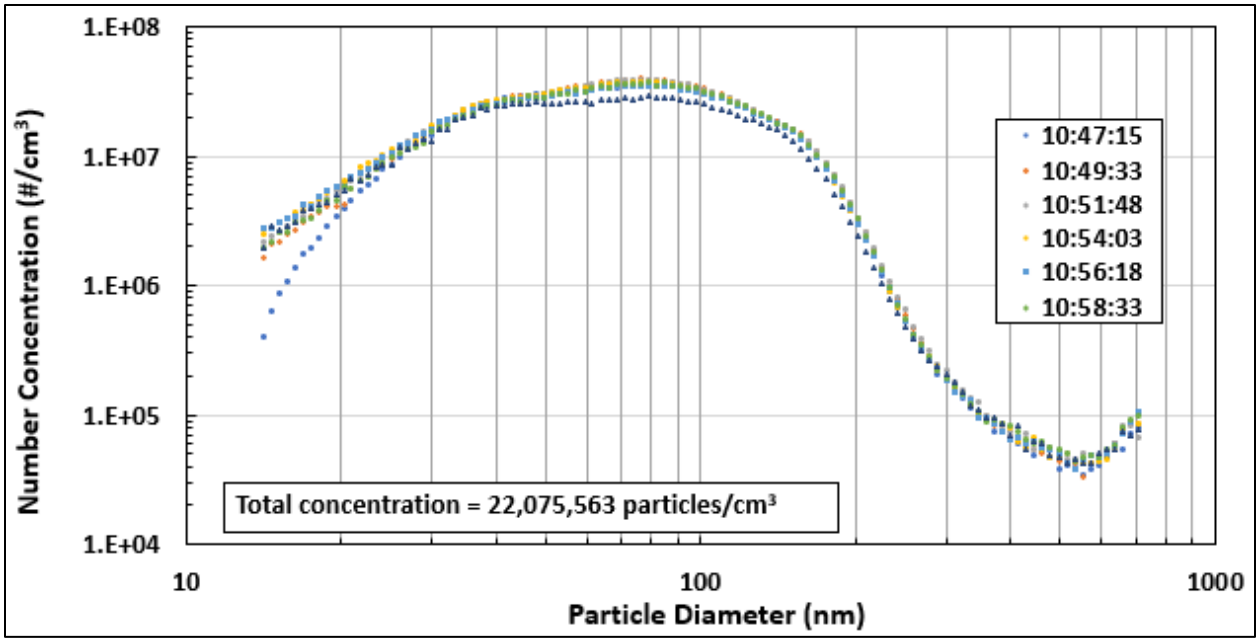

Figure 18b: Flue gas supply aerosol number concentration and size distribution measurements for different samples during operation of two coal boilers (187,000 lb/hr boiler steam rate, date: 2/5/2020, 1,000 scfm flue gas flow)

As shown in Figures 18a-b, aerosol particle concentrations reached peaks near 4E+07 particles/cm^3 for particles between 70-90 nm in size. These peak concentrations are lower than what were observed at Abbott in February 2016 (Figure 4), but still provide a sufficiently high baseline required for meaningful, comprehensive aerosol mitigation testing.

C.2.2 RWE high-velocity water spray-based system pilot testing completed by Linde

Table I summarizes the conditions tested for the RWE high-velocity water spray-based system.

Table I: High-velocity spray tower test conditions

Design Parameter	Range
Water circulation temperature range (°F)	80-130
Water circulation flowrate range (gpm)	100-300
Flue gas volumetric flow range (scfm)	500-1000
Perforated plate type	Medium-size holes, Large-size holes
Spray nozzle type	Type 1, Type 2
Abbott boiler operation	One or two boilers

Aerosol removal efficiency performance figures for the water spray system are shown below. Here, aerosol particle removal efficiency is calculated as:

$$\frac{Inlet\ aerosol\ particle\ number\ concentration\ -\ Outlet\ aerosol\ particle\ number\ concentration}{Inlet\ aerosol\ particle\ number\ concentration} * 100\%$$

where number concentration is measured as # of particles/cm^3 for each recorded particle diameter (nm). Here, data sets in each figure are labeled in the legends according to:
Supply gas volumetric flowrate (in scfm) _Water circulation rate (in gpm)_Water circulation temperature (°F)_Water spray nozzle type_Perforated plate type
N1 & N2 indicate the two different water spray nozzle types tested and LPP & MPP indicate the large-sized hole perforated plate and medium-sized hole perforated plate, respectively, that were used inside the water wash column for vapor-liquid distribution.

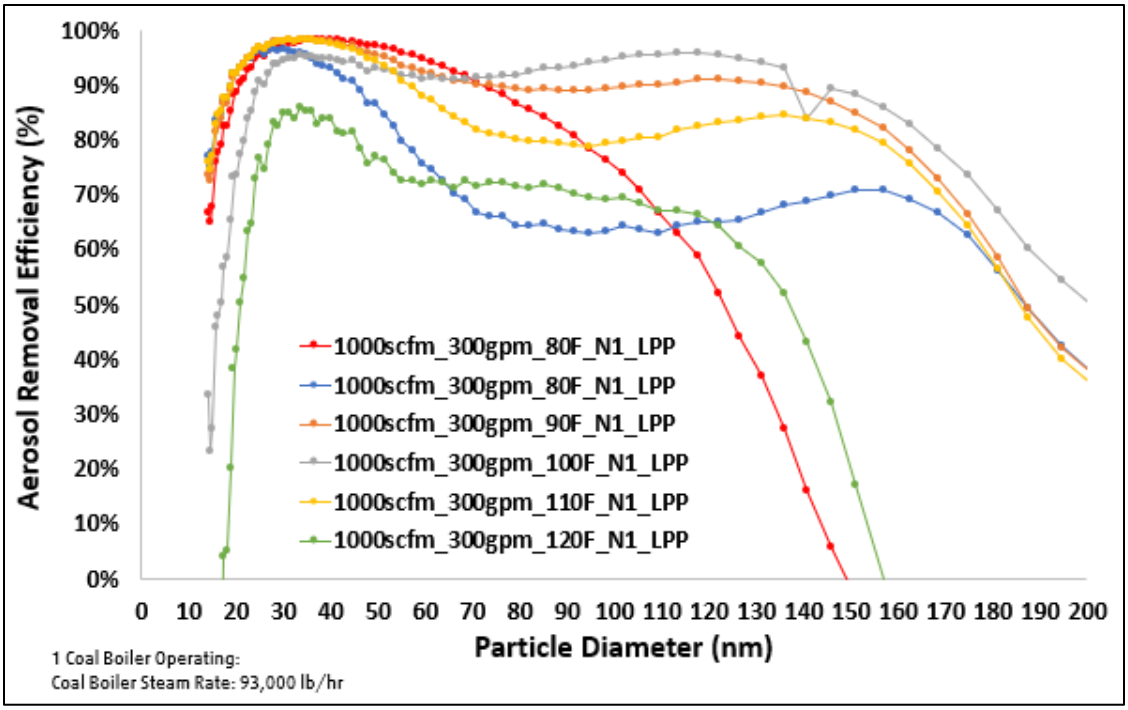

Figure 19: High Velocity Spray Tower Aerosol Removal Performance Results: Effect of Water Circulation Temperature (°F)

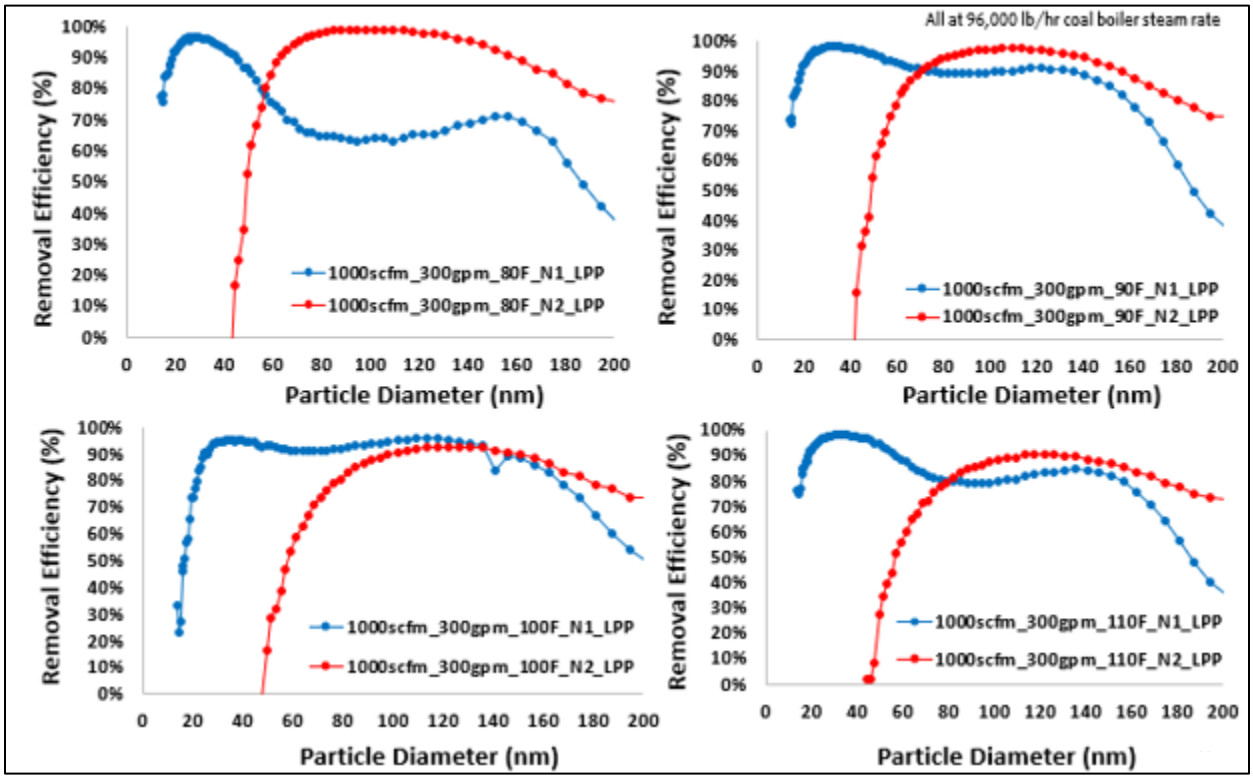

Figure 20a: High Velocity Spray Tower Aerosol Removal Performance Results: Effect of Nozzle Type at Varying Water Circulation Temperature (°F) (N1 = water spray nozzle type 1 and N2 = water spray nozzle type 2)

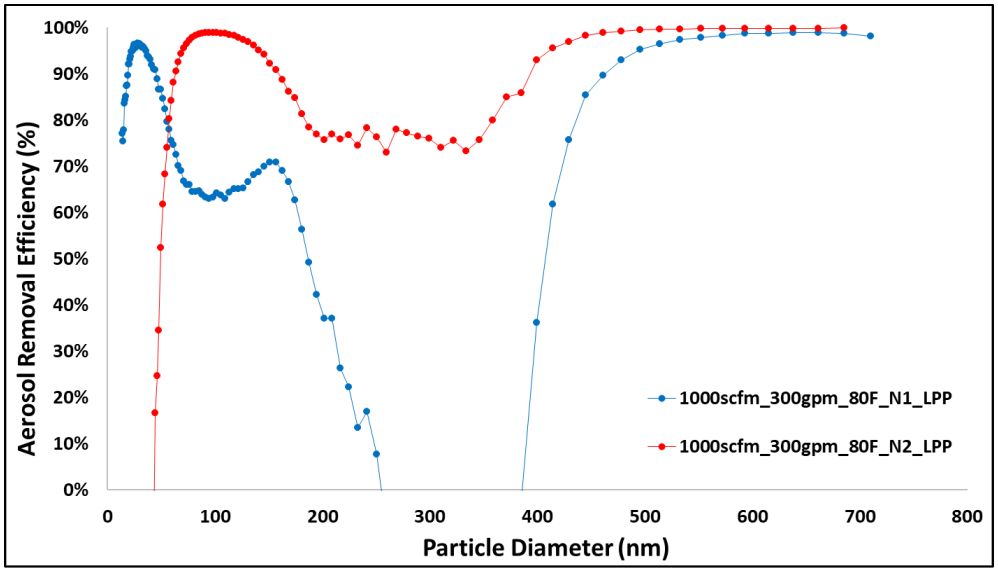
Aerosol Removal Efficiency (%)
100%
90%
80%
70%
60%
50%
40%
30%
20%
10%
0%
0
100
200
300
400
500
600
700
800
Particle Diameter (nm)
1000scfm_300gpm_80F_N1_LPP
1000scfm_300gpm_80F_N2_LPP

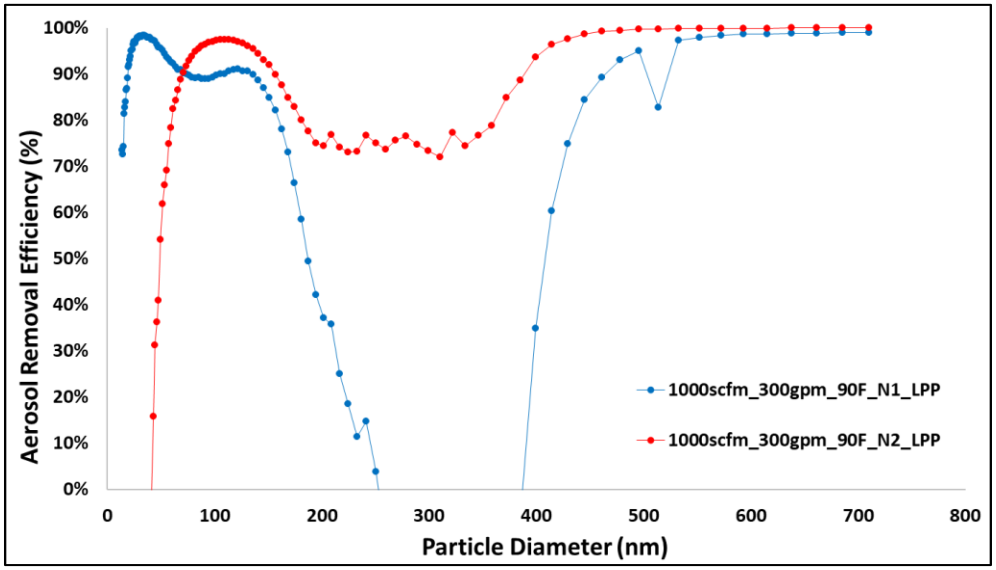
Aerosol Removal Efficiency (%)
100%
90%
80%
70%
60%
50%
40%
30%
20%
10%
0%
0
100
200
300
400
500
600
700
800
Particle Diameter (nm)
1000scfm_300gpm_90F_N1_LPP
1000scfm_300gpm_90F_N2_LPP

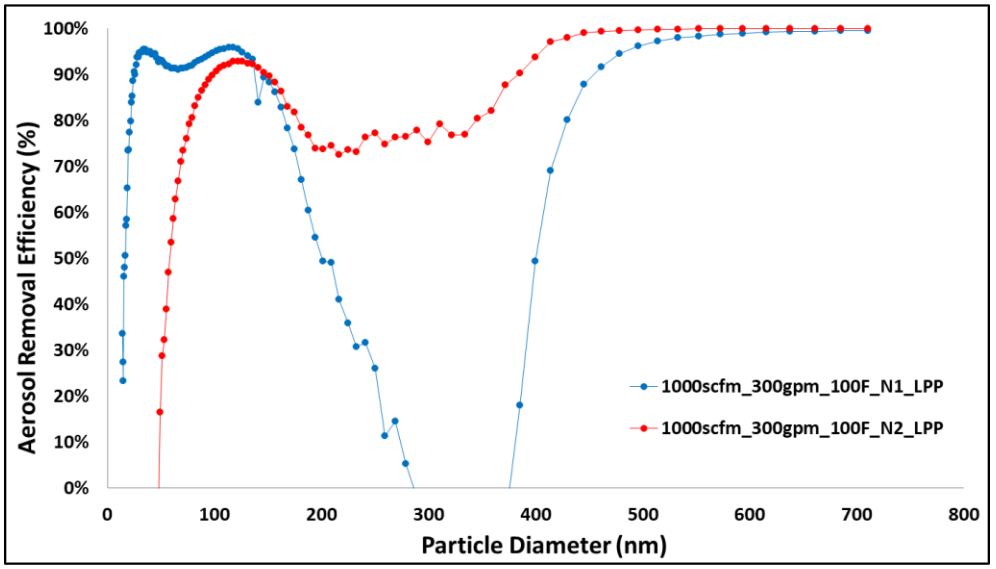
Aerosol Removal Efficiency (%)
100%
90%
80%
70%
60%
50%
40%
30%
20%
10%
0%
0
100
200
300
400
500
600
700
800
Particle Diameter (nm)
1000scfm_300gpm_100F_N1_LPP
1000scfm_300gpm_100F_N2_LPP

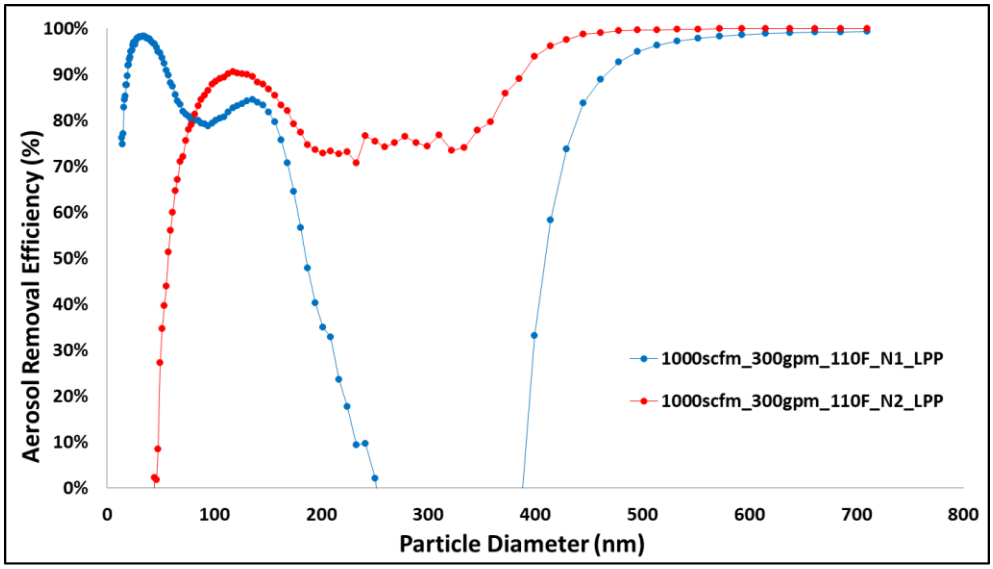

Figure 20b: High Velocity Spray Tower Aerosol Removal Performance Results: Effect of Nozzle Type at Varying Water Circulation Temperature (°F) (N1 = water spray nozzle type 1 and N2 = water spray nozzle type 2)

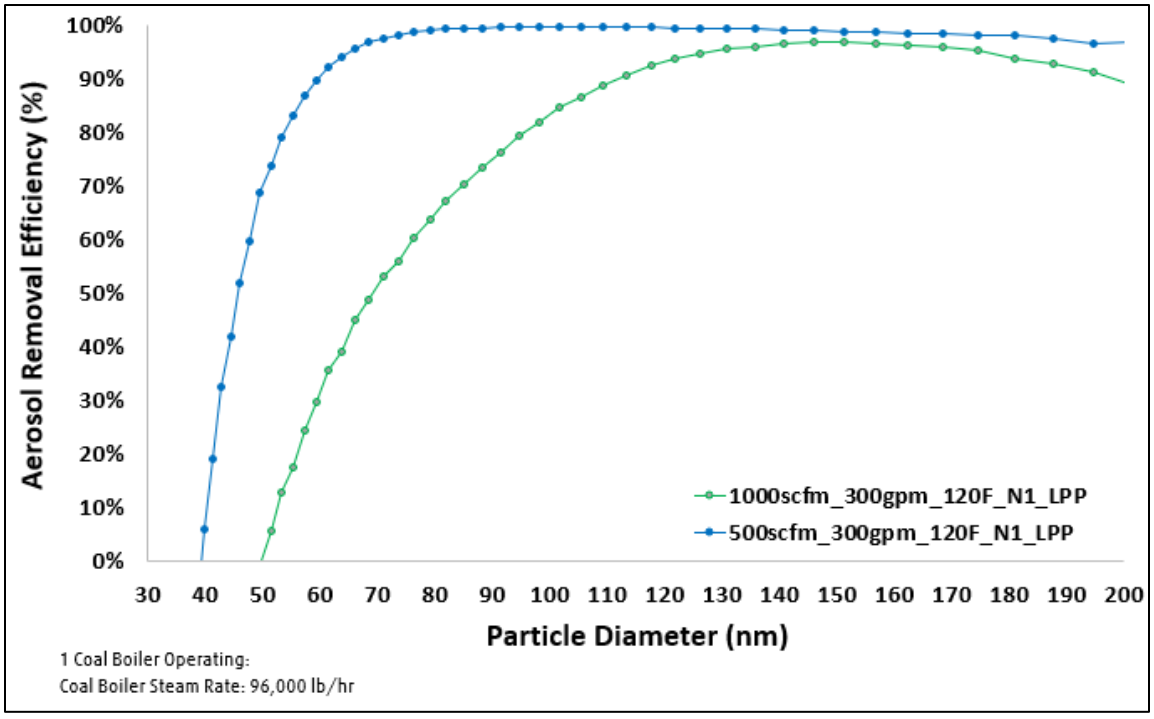

Figure 21: High Velocity Spray Tower Aerosol Removal Performance Results: Effect of Flue Gas Volumetric Flow Rate (scfm)

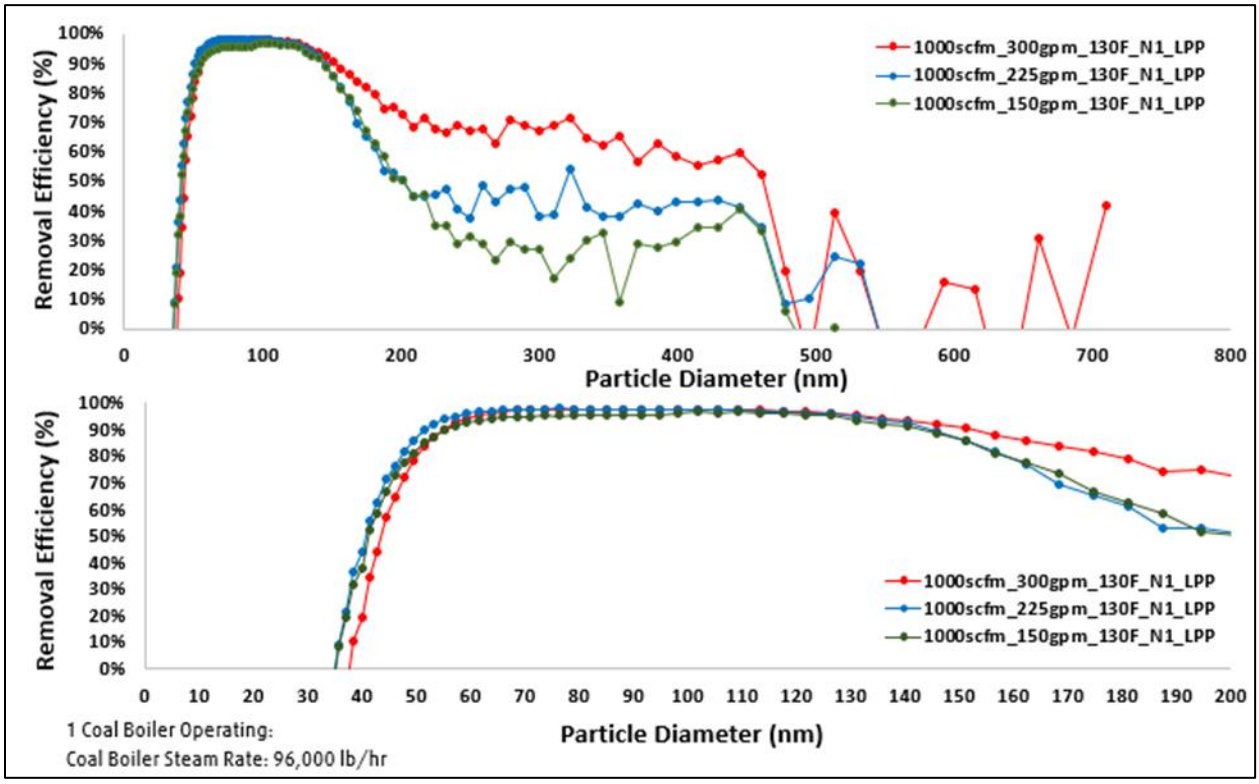

Figure 22: High Velocity Spray Tower Aerosol Removal Performance Results: Effect of Water Circulation Rate (gpm)

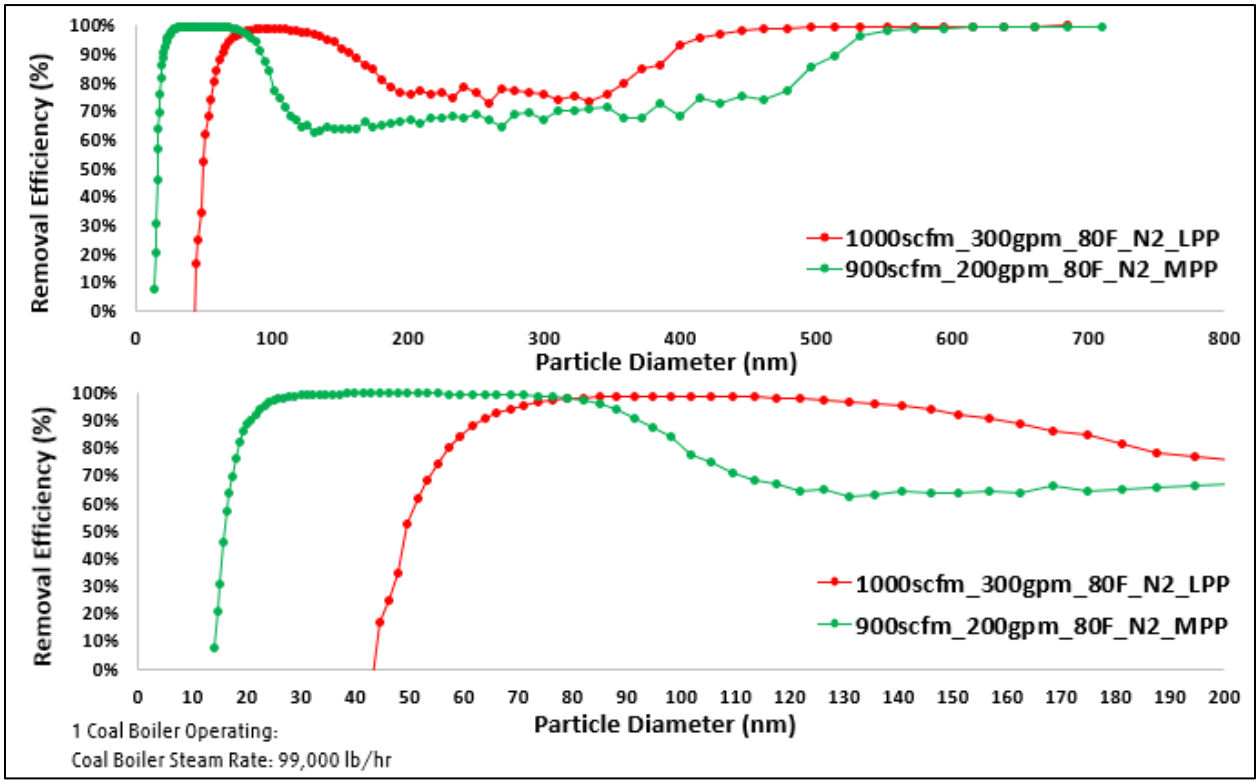

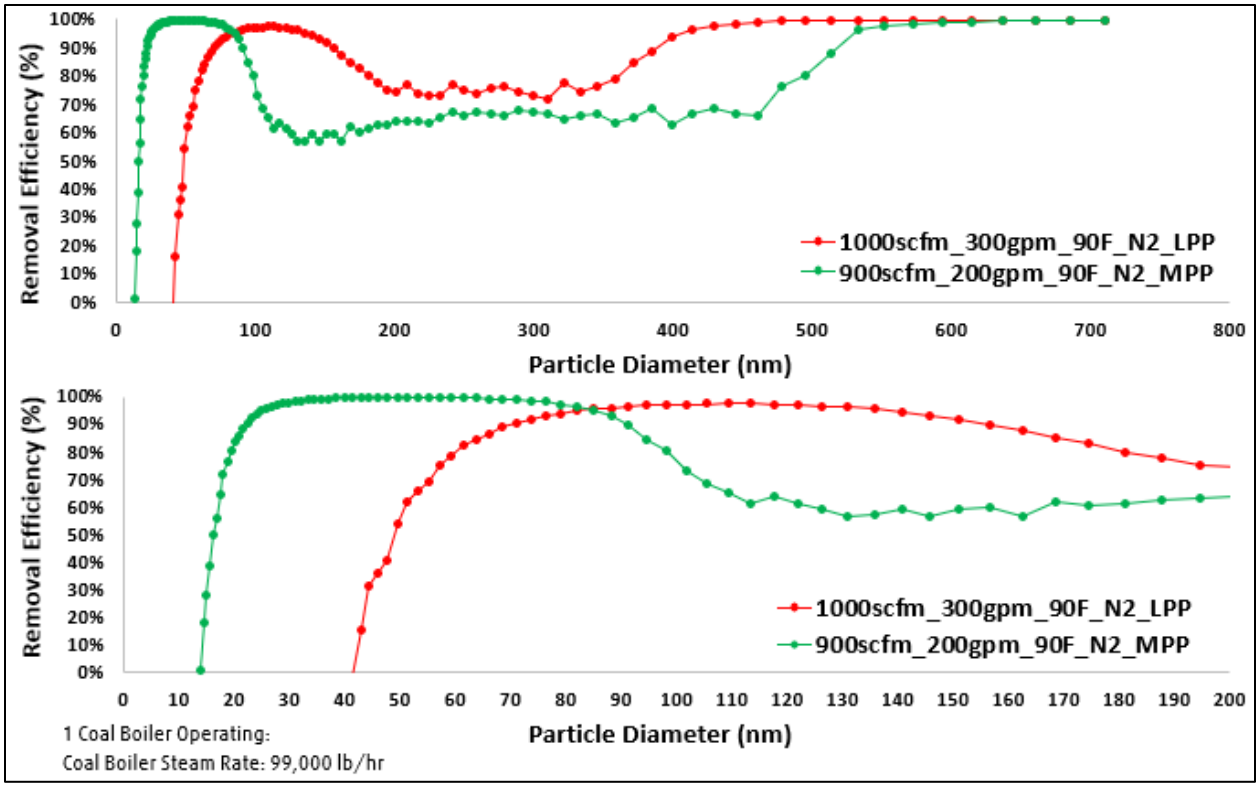
Removal Efficiency (%)
100%
90%
80%
70%
60%
50%
40%
30%
20%
10%
0%
0
100
200
300
400
500
600
700
800
Particle Diameter (nm)
1000scfm_300gpm_90F_N2_LPP
900scfm_200gpm_90F_N2_MPP
Removal Efficiency (%)
0
10
20
30
40
50
60
70
80
90
100
110
120
130
140
150
160
170
180
190
200
Particle Diameter (nm)
1000scfm_300gpm_90F_N2_LPP
900scfm_200gpm_90F_N2_MPP
1 Coal Boiler Operating:
Coal Boiler Steam Rate: 99,000 lb/hr

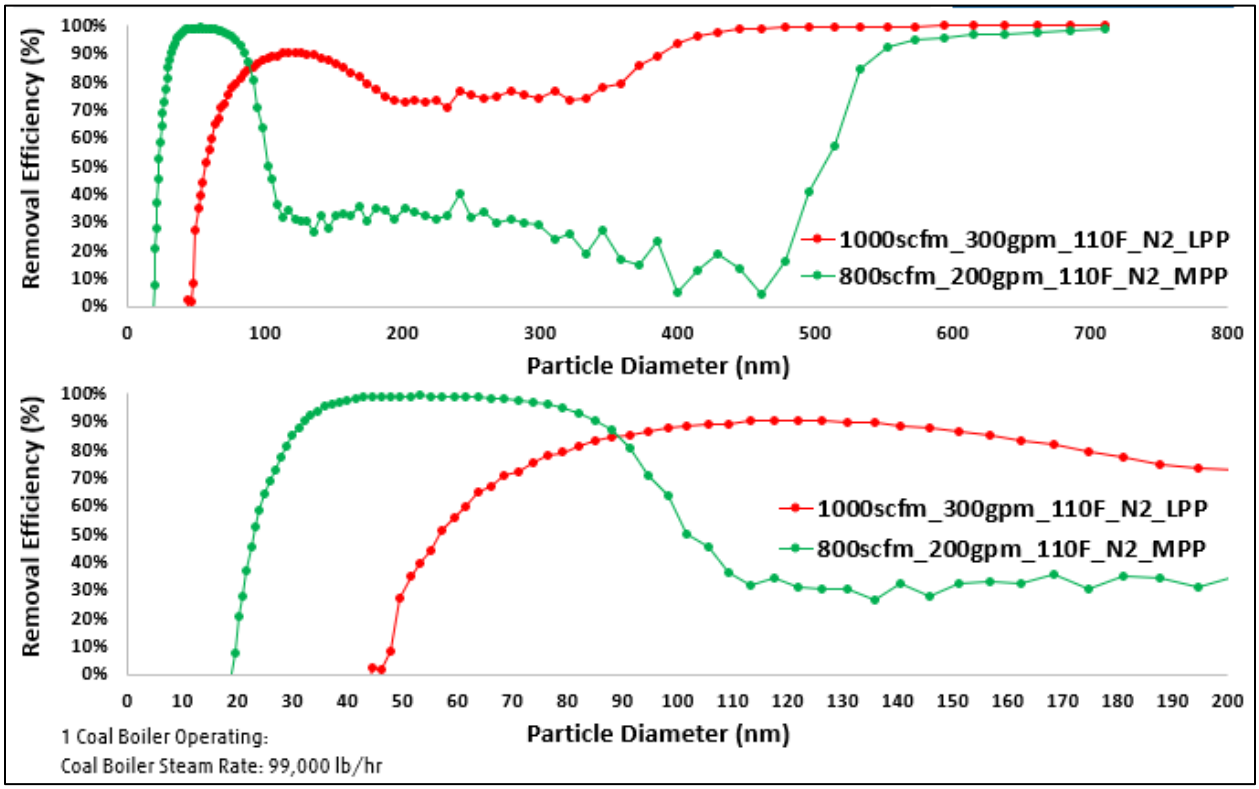
Removal Efficiency (%)
100%
90%
80%
70%
60%
50%
40%
30%
20%
10%
0%
0
100
200
300
400
500
600
700
800
Particle Diameter (nm)
1000scfm_300gpm_110F_N2_LPP
800scfm_200gpm_110F_N2_MPP
Removal Efficiency (%)
0
10
20
30
40
50
60
70
80
90
100
110
120
130
140
150
160
170
180
190
200
Particle Diameter (nm)
1000scfm_300gpm_110F_N2_LPP
800scfm_200gpm_110F_N2_MPP
1 Coal Boiler Operating:
Coal Boiler Steam Rate: 99,000 lb/hr

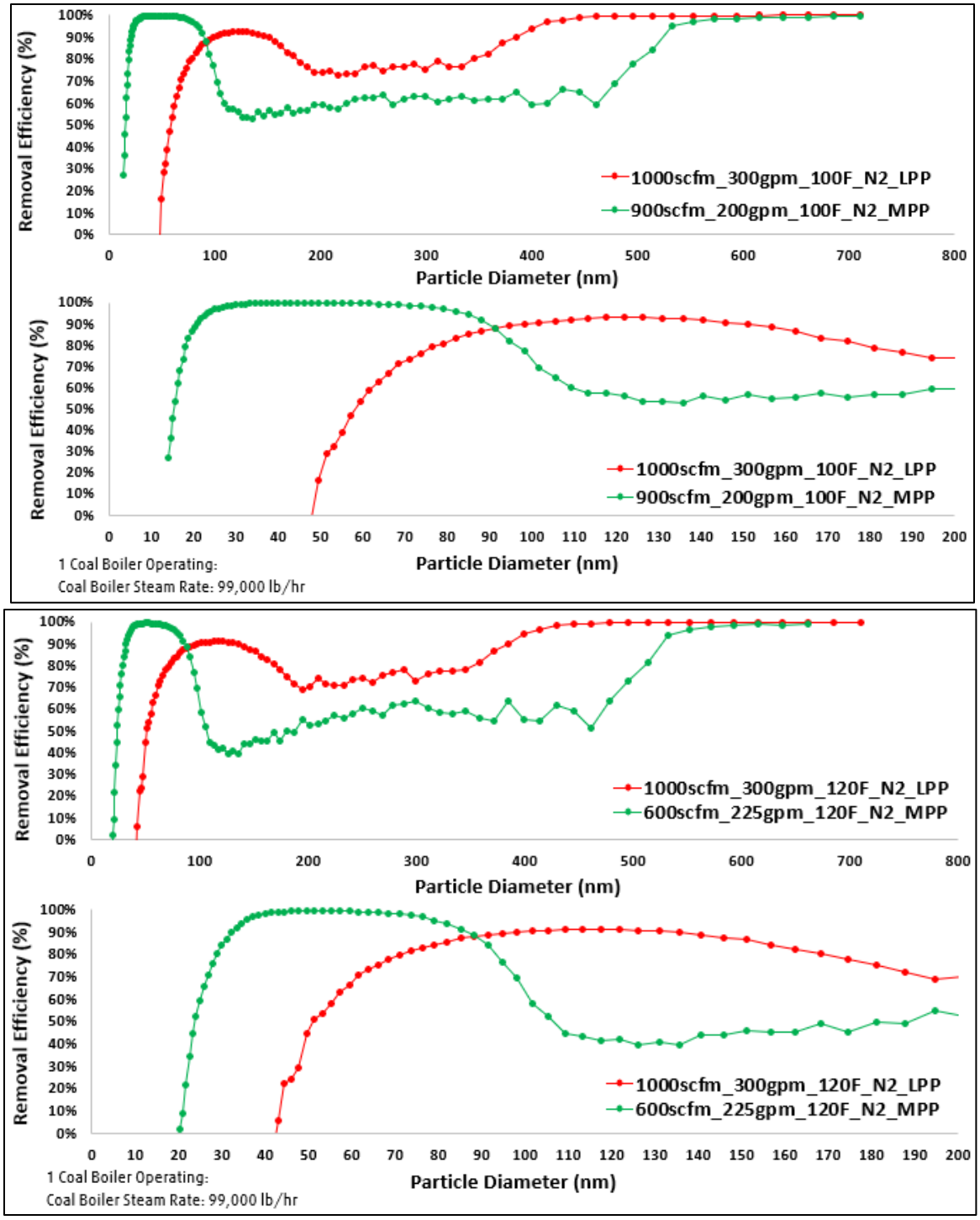

Figure 23: High Velocity Spray Tower Aerosol Removal Performance Results: Effect of Perforated Plate Type at Varying Temperatures (°F) LPP = large-size holes perforated plate, MPP = medium-sized holes perforated plate, N2 = water spray nozzle type 2

Figure 19 indicates that water circulation temperatures between 90 and 110°F provide the highest removal efficiencies for particle sizes between 20 and 200 nm, with 100°F providing the best overall efficiencies for particles greater than 70 nm in size. For the 90-100°F temperature range, removal efficiency can reach above 95% for 20-60 nm particles and roughly averages at or above 90% from 20-140 nm particle size, after which it begins to decrease, averaging close to ~65% efficiency for 180-200 nm sized particles. This data set used the N1 nozzle type and large-sized hole perforated plate, which both impact removal efficiency performance for particles less than 200 nm in diameter. It should be noted that the reference supply flue gas condition can change throughout the day and that the efficiency measurements are relative to this reference, which was collected once on the day this entire data set was measured. The reason is that the project team did not have duplicate aerosol measurement equipment to simultaneously measure inlet and outlet aerosol number concentrations, but the daily averages provide a best-case estimate for analysis purposes. The power plant operating conditions such as steam rate also did not vary significantly each day, and supply measurements were repeated several times each day to verify that supply conditions had not changed. Instantaneous variations in the supply conditions do account for some differences in the efficiency calculations, as illustrated with the second 80°F data set showing the large efficiency deviation for particles larger than 80 nm compared to the first 80°F data set.

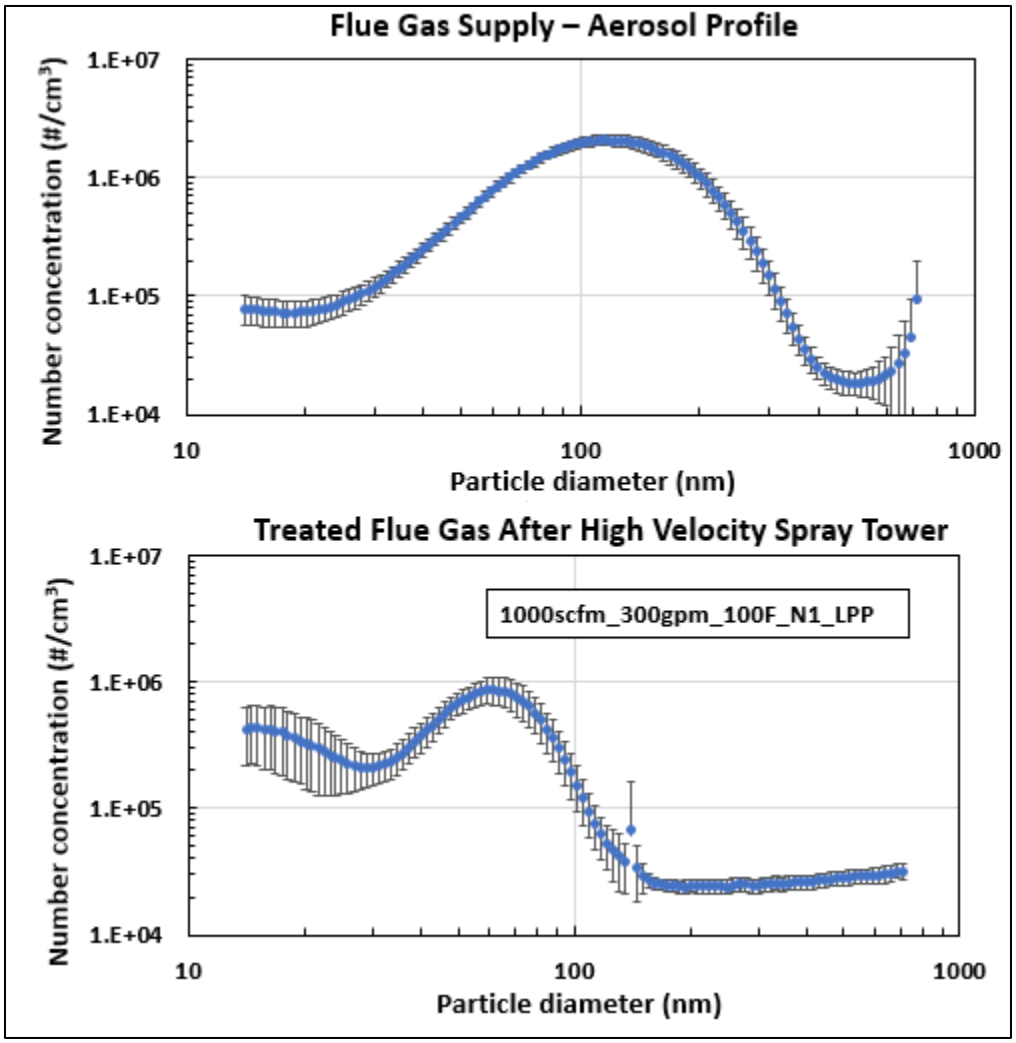

Figure 24: Particle number concentration and size distribution profile before and after high velocity spray tower with statistical error bars based on data from 26 separate data sets (1000scfm_300gpm_100F_N1_LPP data set shown)

Figure 24 illustrates the significant effect that the spray tower has on aerosol number concentrations in the 70-200 nm size range for the 1000scfm_300gpm_100F_N1_LPP data set, which was averaged from 26 individual test runs over the course of an hour. The removal efficiencies for each particle size range for this data set are listed in Table II, showing that an average of ~87% removal efficiency is achieved in the 70-200 nm size range. Based on extensive prior testing of the Linde-BASF PCC technology and its environmental performance, aerosol particles larger than 200 nm that have potential for solvent carryover are typically captured by a demister placed at the top of the absorber column. Hence, the reduced aerosol removal efficiency observed for particle sizes above 200 nm shown in Table II (in the range of 209.1 to 250.3 nm specifically) will be mitigated by enhanced particle control provided by the absorber demister used in the Linde-BASF design.

Table II: High-velocity spray tower removal efficiency using N1 and LPP at 100°F water circulation temperature

Particle Size Range (nm)	Average Aerosol Removal Efficiency (%)
20.2 to 30	86.94%
31.1 to 40	95.04%
41.4 to 51.4	93.61%
53.3 to 63.8	91.64%
66.1 to 82	91.59%
85.1 to 101.8	93.98%
105.5 to 126.3	95.49%
131 to 162.5	88.23%
168.5 to 201.7	63.88%
209.1 to 250.3	35.71%
Overall from 70 to 200 nm	86.55%

Figures 20a and 20b show a clear difference in aerosol removal efficiency for nozzle type 1 vs. type 2. For most water circulation temperatures in the range of 80-120°F, nozzle type 1 provides greater removal efficiency for particles sizes below 50 nm compared to type 2. Type 2 provides higher efficiency for particles greater than 85 nm for 3 out of 4 temperature cases and the efficiency benefits for type 2 increase substantially for particle sizes greater than 200 nm. This comparison indicates that a combination of the design features from nozzle type 1 and type 2 could help optimize removal efficiency to enable efficiencies greater than 90% in the 70-200 nm particle size range for a full range of temperature and process operating conditions. Table III quantifies the aerosol removal efficiencies using N1 compared to N2. For the LPP, the N2 design provides the best removal efficiency for the spray tower at 91.6%.

Table III: High-velocity spray tower removal efficiency using nozzle type 1 (N1) and nozzle type 2 (N2) with LPP at varying water circulation temperatures (°F)

Particle Size Range (nm)	N1 - Average Aerosol Removal Efficiency (%)	N2 - Average Aerosol Removal Efficiency (%)
90°F Water Circulation Temperature		
53.3 to 63.8	92.93%	75.81%
66.1 to 82	90.02%	91.26%
85.1 to 101.8	89.19%	96.48%
105.5 to 126.3	90.53%	97.21%
131 to 162.5	85.86%	92.60%
168.5 to 201.7	54.42%	79.14%
70 to 200 nm	81.80%	91.62%
100°F Water Circulation Temperature		
53.3 to 63.8	91.64%	48.80%
66.1 to 82	91.59%	75.75%
85.1 to 101.8	93.98%	88.07%
105.5 to 126.3	95.49%	92.32%
131 to 162.5	88.23%	90.10%
168.5 to 201.7	63.88%	77.89%

70 to 200 nm	86.55%	85.76%
110°F Water Circulation Temperature		
53.3 to 63.8	89.02%	52.59%
66.1 to 82	81.65%	74.87%
85.1 to 101.8	79.41%	85.94%
105.5 to 126.3	82.01%	89.91%
131 to 162.5	81.85%	87.29%
168.5 to 201.7	52.46%	76.62%
70 to 200 nm	75.34%	83.72%

Figure 21 indicates the significant effect that the ratio of flue gas flow to water circulation flow has on particle removal efficiency in the 70-200 nm size range of interest. Increasing the water circulation rate relative to the flue gas flow rate clearly improves removal efficiency but comes at the cost of higher electrical power consumption for the circulation pump for continuous operations. Figure 22 indicates this same effect, where water circulation rate is varied relative to flue gas flow rate. Figure 22 shows a pronounced effect on removal efficiency only for particle sizes greater than 140 nm, indicating that circulation rate could be optimized based on both pump electrical consumption and the reduction in solvent losses due to aerosol pretreatment.

Figure 23 demonstrates the impact of perforated plate design on aerosol removal efficiency. The medium-sized hole perforated plate (MPP) caused water build-up on the plate due to a lack of efficient liquid distribution. This resulted in excessively high pressure drop across the spray tower that the flue gas blower could not overcome. Hence, the flue gas flow rates shown for the MPP cases are the maximum flow that could be achieved at the given conditions. This limitation clearly shows that the perforated plate design must be carefully evaluated to prevent unnecessary flue restriction through the tower. Even with this difference in comparison, the large-sized hole perforated plate (LPP) provides removal efficiencies between 70 and 90% for particle sizes between 70 and 200 nm. Likely due to the water buildup on the plate, the MPP does provide high aerosol removal efficiencies >90% in the 10-60 nm particle size range.

Regarding contaminant removal, Figure 25 shows that the water spray tower can achieve ~68% SO_2 removal efficiency relative to the supply flue gas. The supply gas had an average SO_2 content of 43 ppmv during the period when this data was collected. This performance indicates that, even without adding caustic solution, as would be done for a direct contact cooling system upstream of a PCC plant absorber, the spray tower offers substantial SO_2 removal even at ambient pressure (1 atm).

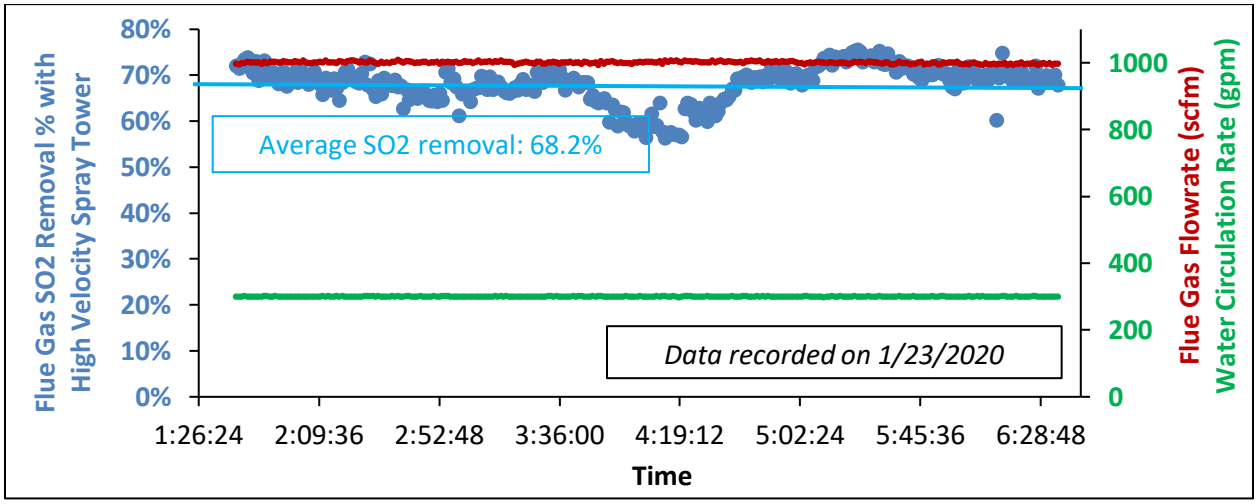

Figure 25: Representative SOx removal efficiency data for high-velocity spray tower at typical conditions (1000 scfm flue gas flowrate and 300 gpm water circulation rate)

C.2.3 Advanced WUSTL ESP system testing

C.2.3a WUSTL ESP aerosol efficiency tests using air with NaCl & ash at ACERF

The advanced ESP was tested at on aerosol particles with ambient air at WUSTL's Advanced Coal and Energy research Facility (ACERF) to evaluate its performance at controlled operating conditions. The objective was to evaluate the performance of the PI-ESP's collection efficiency as a function of particle size, particle velocity, charging voltage in the presence and absence of soft X-rays. Two aerosol types were used for testing: (i) NaCl and (ii) Ash. NaCl aerosols were used because they are stable operationally, and ash was used to replicate the real system. NUCON pneumatic aerosol generator was used to generate NaCl aerosols, while a custom-built fluidization system was used to generate ash aerosols from previously collected and sieved dry fly ash. The aerosol source was diluted with room air such that the total flow through the PI-ESP is in the desired range. The experimental plan is shown in Table IV. The results obtained from the testing are shown in Figures 26(a) – 26(f).

Table IV: Experimental plan for testing the 500 scfm PI-ESP at ACERF

Section	Range/condition	Description
I-V Characteristics	Steady air flow at 500 scfm with and without soft X-rays	Compare the corona inception voltage and absolute values of current
Effect of charging stage voltage	Air flow rate: 300 – 700 scfm Charging stage voltage: 5 – 8 kV Aerosol number concentration: 5 x 10^5 #/cm^3 NaCl aerosol	Investigate the influence of charging stage voltage on collection efficiency at different operating conditions.
Effect of total number concentration	Air flow rate: 500 scfm, Charging stage voltage: 5 – 8 kV Aerosol number concentration: (0.5 - 50) x 10^5 #/cm^3 NaCl aerosol	Investigate the influence of aerosol number concentration on collection efficiency at different operating conditions.
Effect of soft X-rays	Air flow rate: 300 – 700 scfm Charging stage voltage: 5 – 8 kV aerosol number concentration: (0.5 - 50) x 10^5 #/cm^3 NaCl aerosol	Investigate the influence of soft X-rays on collection efficiency at different operating conditions to establish conditions at which soft X-rays enhance collection efficiency.
Effect of air flow rate	Air flow rate: 300 – 700 scfm Charging stage voltage: 5 – 8 kV aerosol number concentration: 5 x 10^5 #/cm^3 NaCl aerosol	Investigate the influence of air flow rate and thereby the particle velocity on collection efficiency at different operating conditions.
Effect of aerosol chemical composition	Air flow rate: 500 scfm Charging stage voltage: 5 – 8 kV Aerosol number concentration: (0.5 - 50) x 10^5 #/cm^3 NaCl and fluidized ash aerosol	Investigate the influence of aerosol chemical composition on collection efficiency at different operating conditions.

I-V characteristics:

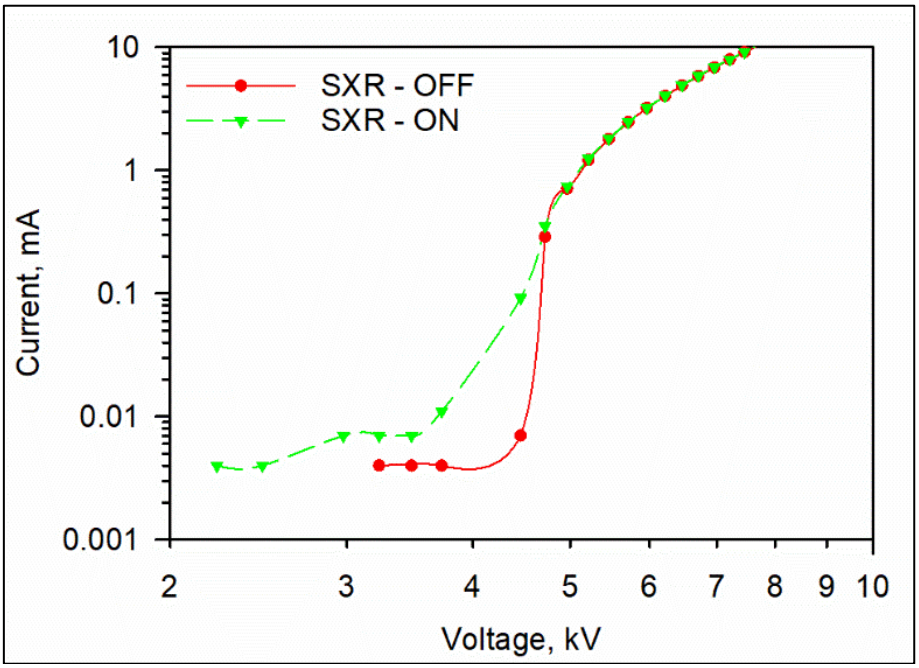

Figure 26(a): I-V curves measured in the presence and absence of soft X-rays.

The I-V characteristics measured at a steady state air flow rate of 500 cfm is shown in Figure 26(a). The IV characteristics were studied in the presence and absence of soft X-rays (SXRs). The corona on-set voltage was higher when the SXRs were OFF and the increase in current was smooth in the presence of SXRs. The absolute values of current were higher when SXRs were ON. These results show demonstrate that the SXRs effectively increased the concentration of charged ions.

Effect of Charging stage voltage and aerosol number concentration on collection efficiency:

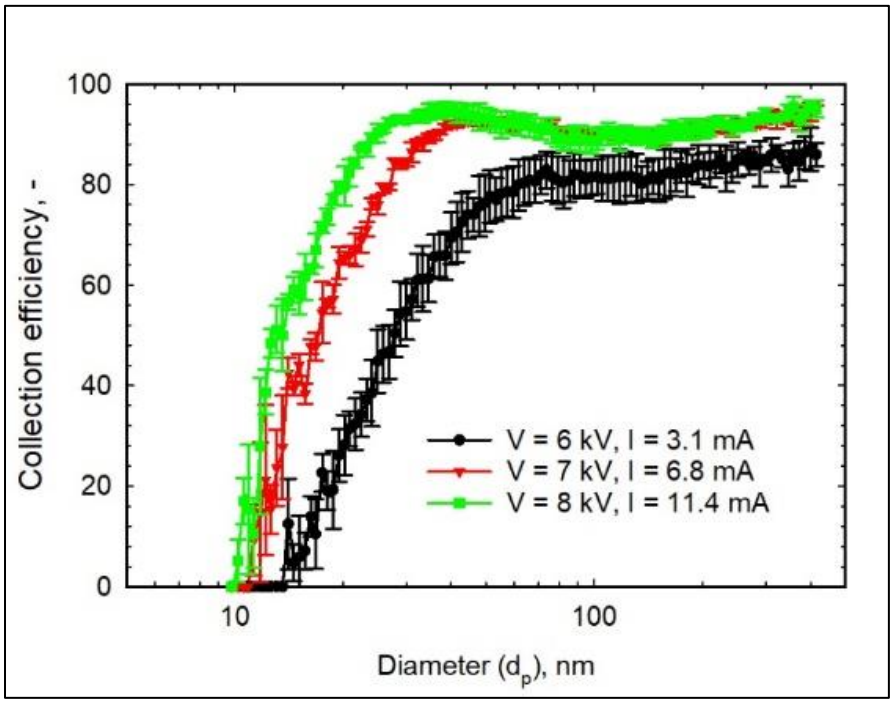

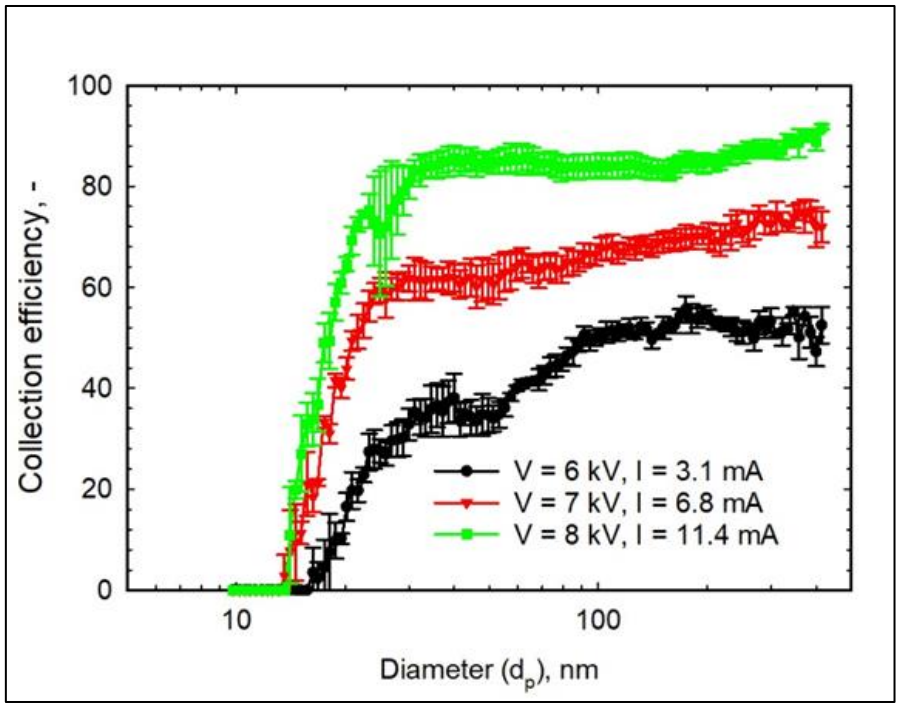

Figure 26(b): Effect of charging stage voltage on collection efficiency for NaCl aerosol at 500 scfm flow and aerosol number concentration of 5 x 10^5 #/cm^3 (upper chart) and 5 x 10^6 #/cm^3 (lower chart)

The effect of charging stage voltage on collection efficiency is shown in Figure 26(b). The highest collection efficiency was observed at the highest charging stage voltage. The collection efficiency showed a monotonic increase for the size range between 20 – 40 nm and was mostly constant at particle sizes greater than 40 nm.

Effect of soft X-rays on collection efficiency:

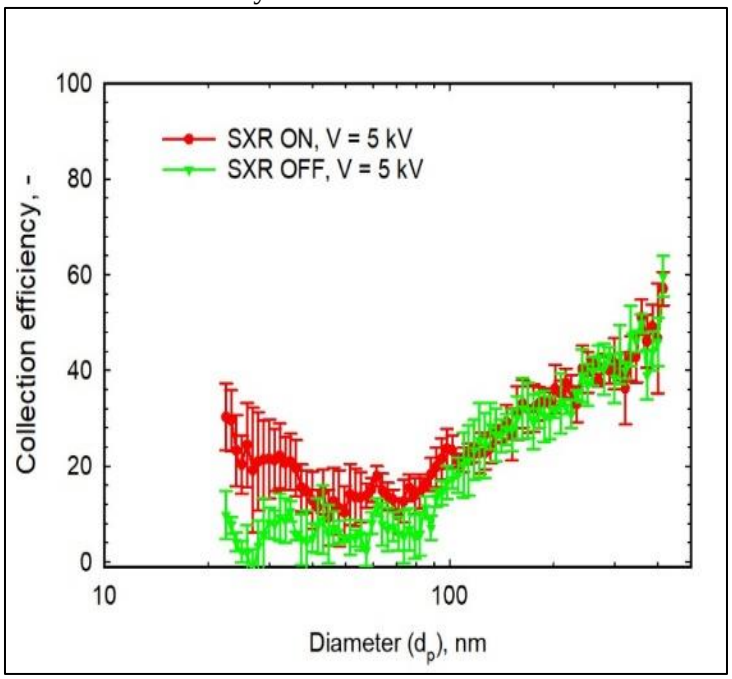

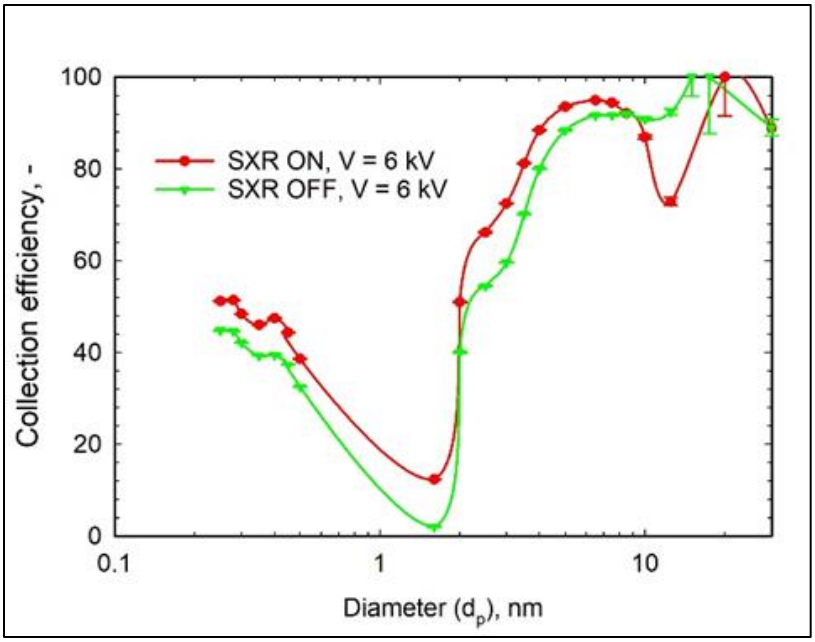

Figure 26(c): Effect of soft X-ray on collection efficiency at aerosol number concentrations of 5 x 10^5 #/cm^3 for NaCl aerosol (upper chart) and ash aerosol (lower chart)

The effect of SXRs on collection efficiency is shown in Figure 26(c). SXRs increased collection efficiencies at lower voltages. Similar observations were observed with NaCl and ash aerosols. At higher voltages it was challenging to differentiate the increase in collection efficiencies due to issues such as ion induced nucleation and non-neutral challenge aerosols.

Effect of gas flow rate on collection efficiency:

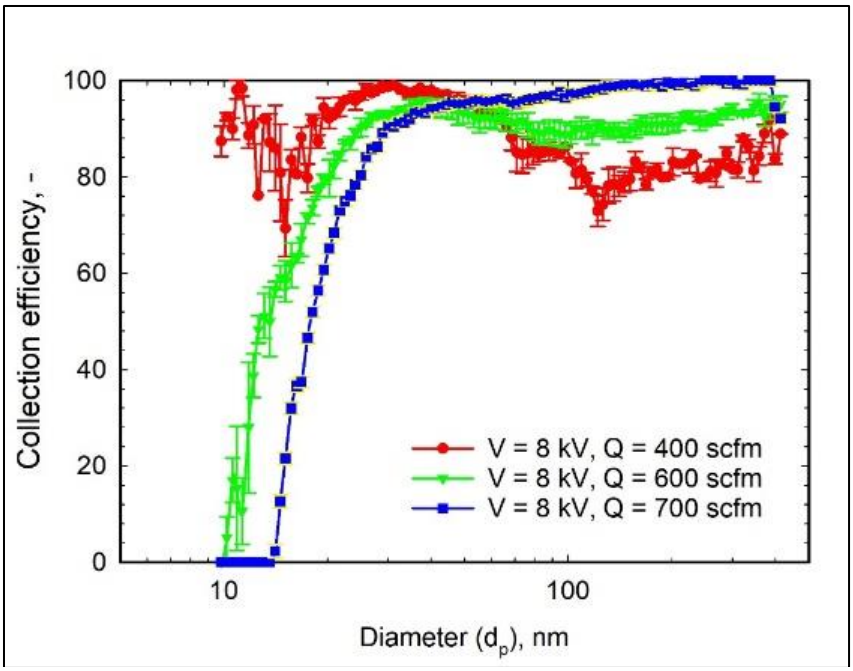

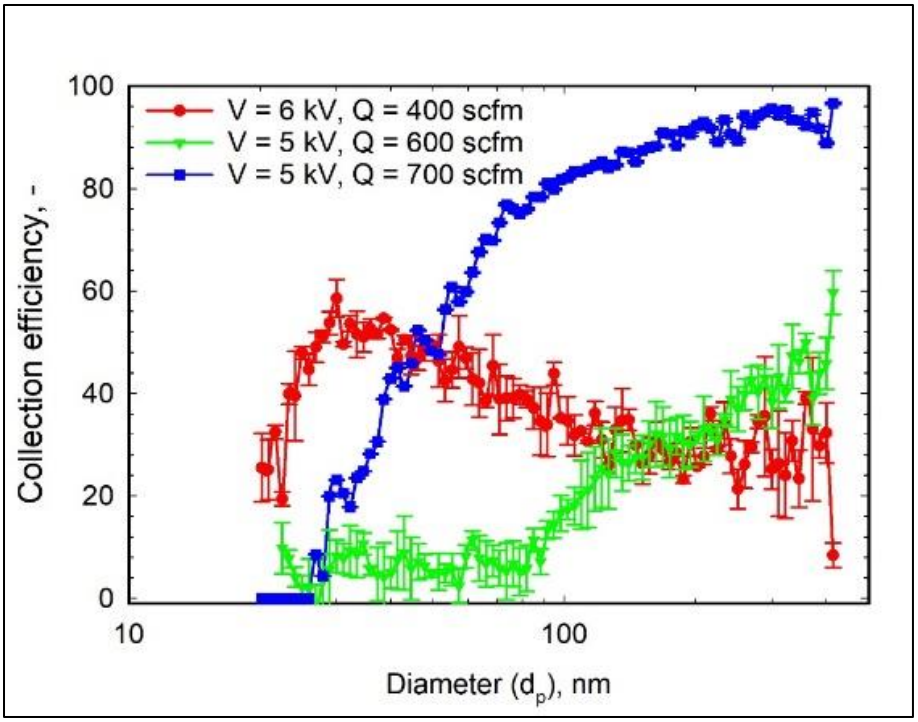

Figure 26(d): Effect of charging stage voltage on collection efficiency for NaCl aerosol at 500 scfm flow and aerosol number concentration of 5 x 10^5 #/cm^3 (upper chart) and 5 x 10^6 #/cm^3 (lower chart)

The effect of gas flow rate on collection efficiency was studied and it was found that the collection efficiency decreased for smaller particles (<40 nm) and increased for larger particles.

C.2.3b WUSTL ESP pilot testing at the Abbott Power Plant

The two-staged Photoionization WUSTL's ESP system was pilot tested at the Abbott Power Plant on actual coal-fired flue gas for several days adjusting operating conditions for the charging and collection stages. The different operating conditions tested are summarized in Table V:

Table V: Pilot plant test operating conditions

Section	Range/condition	Description
Effect of charging stage voltage	Air flow rate: 300, 400, 500, 600 scfm Charging stage voltage: 5, 6, 7, 7.5, 7.75, 8 kV	Investigate the influence of charging stage voltage on collection efficiency at different operating conditions.
Effect of Soft X-Rays	Air flow rate: 500, 600 scfm Charging stage voltage: 5, 6 kV	Investigate the influence of soft X-rays on collection efficiency at different operating conditions to establish conditions at which soft X-rays enhance collection efficiency.
Effect of air flow rate	Air flow rate: 300, 400, 500, 600 scfm, Charging stage voltage: 5, 6, 7, 7.5, 7.75, 8 kV	Investigate the influence of air flow rate and thereby the particle velocity on collection efficiency at different operating conditions.

The ESP was operated at charging stage voltages ranging between 5 – 8 kV and the current in the charging stage ranged between 1 – 9 mA. The flow rate of the flue gas to the ESP was set between 300 – 500 scfm by adjusting the blower's speed. The collection stage was operated at a constant current and voltage. The collection efficiencies obtained at these operating conditions are plotted on Figures 27 – 32. Figures 27 and 28 show the repeatability of the measured collection efficiency at 300 scfm, Figures 29 and 30 show the repeatability of the measured collection efficiency at 400 scfm, and Figures 30 and 31 show repeatability in measurements at 500 scfm. The collection efficiencies were the highest at 500 scfm and is expected as the ESP was designed to operate at 500 scfm. The maximum efficiencies (~ 80 %) were obtained at the highest charging stage voltage (7.75 kV). For most cases, collection efficiency showed a maximum at around 300 nm and was poor for particle sizes below 30 nm. While similar profiles were observed in the size dependent collection efficiencies, the absolute values of the collection efficiency increased with increasing charging stage voltages.

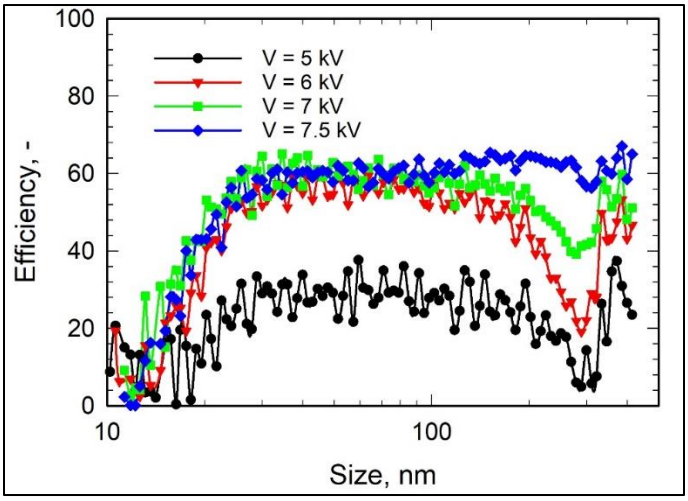

Figure 27:
ESP test conditions:
Flue gas flowrate: 300 scfm
Aerosol particle concentration: 2 x 10^7 #/cm^3
Single coal-fired boiler operation
(~100,000 lb/hr steam rate)
Voltage shown is charging stage voltage (kV)

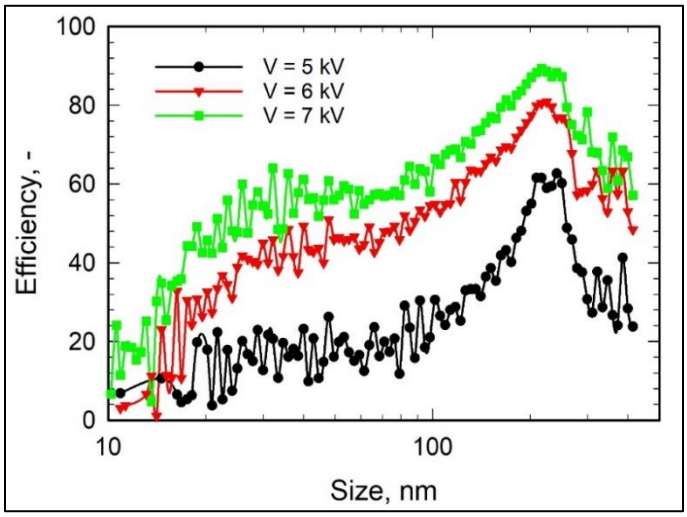

Figure 28:
ESP test conditions:
Flue gas flowrate: 300 scfm (repeat)
Aerosol particle concentration: 2 x 10^7 #/cm^3
Single coal-fired boiler operation
(~100,000 lb/hr steam rate)
Voltage shown is charging stage voltage (kV)

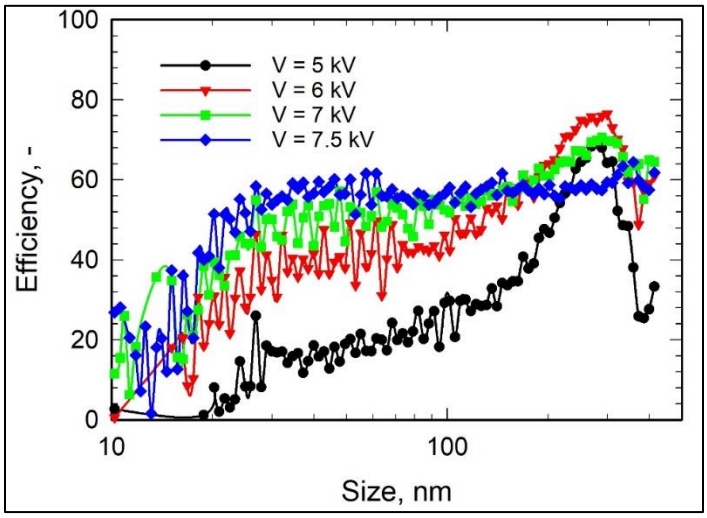

Figure 29:
ESP test conditions:
Flue gas flowrate: 400 scfm
Aerosol particle concentration: 2 x 10^7 #/cm^3
Single coal-fired boiler operation
(~100,000 lb/hr steam rate)
Voltage shown is charging stage voltage (kV)

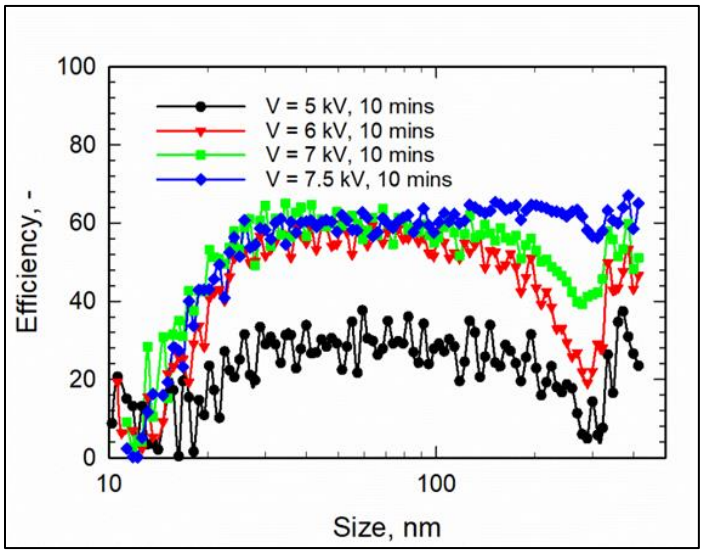

Figure 30:
ESP test conditions:
Flue gas flowrate: 400 scfm (repeat)
Aerosol particle concentration: 2 x 10^7 #/cm^3
Single coal-fired boiler operation
(~100,000 lb/hr steam rate)
Voltage shown is charging stage voltage (kV)
Test duration shown

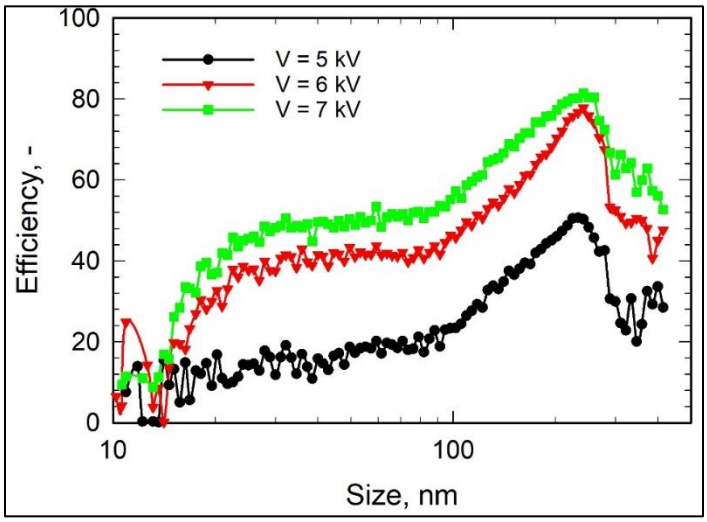

Figure 31:
ESP test conditions:
Flue gas flowrate: 500 scfm
Aerosol particle concentration: 2 x 10^7 #/cm^3
Single coal-fired boiler operation
(~100,000 lb/hr steam rate)
Voltage shown is charging stage voltage (kV)

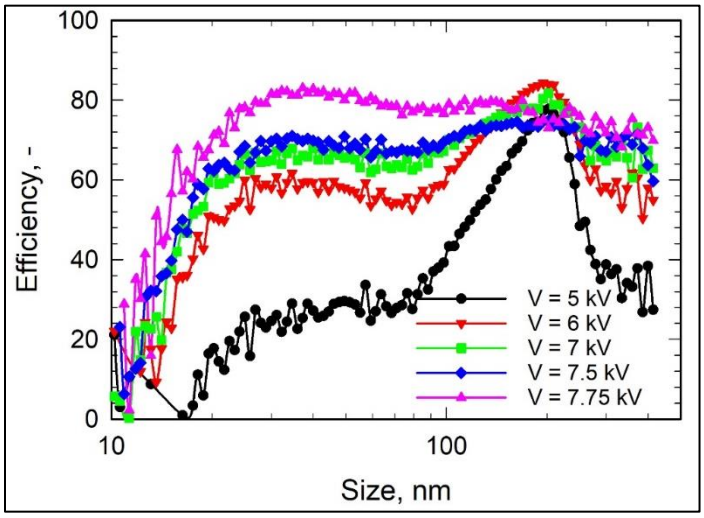

Figure 32:
ESP test conditions:
Flue gas flowrate: 500 scfm (repeat)
Aerosol particle concentration: 2 x 10^7 #/cm^3
Single coal-fired boiler operation
(~100,000 lb/hr steam rate)
Voltage shown is charging stage voltage (kV)

A summary of the average aerosol removal efficiencies for the ESP at various particle sizes and flue gas flowrates is shown in Table VI.

Table VI: Approximate average aerosol removal efficiency of the PI-ESP at Abbott Power Plant Conditions

Flue gas flow rate (scfm)	ESP charging stage voltage (kV)	Size range (nm)	Aerosol removal efficiency (%)
300	7	<40	30%
		40-70	60%
		70-200	**56%**
		>200	48%
	6	<40	25%
		40-70	56%
		70-200	**48%**
		>200	37%
	5	<40	12%
		40-70	29%
		70-200	**28%**
		>200	20%
400	7	<40	32%
		40-70	63%
		70-200	**58%**
		>200	50%
	6	<40	28%
		40-70	58%
		70-200	**51%**
		>200	41%
	5	<40	21%
		40-70	33%
		70-200	**33%**
		>200	24%
500	7	<40	38%

		40-70	67%
		70-200	**73%**
		>200	72%
	6	<40	30%
		40-70	57%
		70-200	**68%**
		>200	66%
	5	<40	21%
		40-70	26
		70-200	**51%**
		>200	45%

Influence of ESP voltage in SO_2 concentration in the flue gas:
In order to investigate the effect of ESP voltage on gas phase SO_2 concentration, the SO_2 concentration measured using FTIR is plotted for a ~14.5-hour period along with ESP charging stage voltage and is shown in Figure 33. It was found that the ESP voltage did not affect SO_2 concentration.

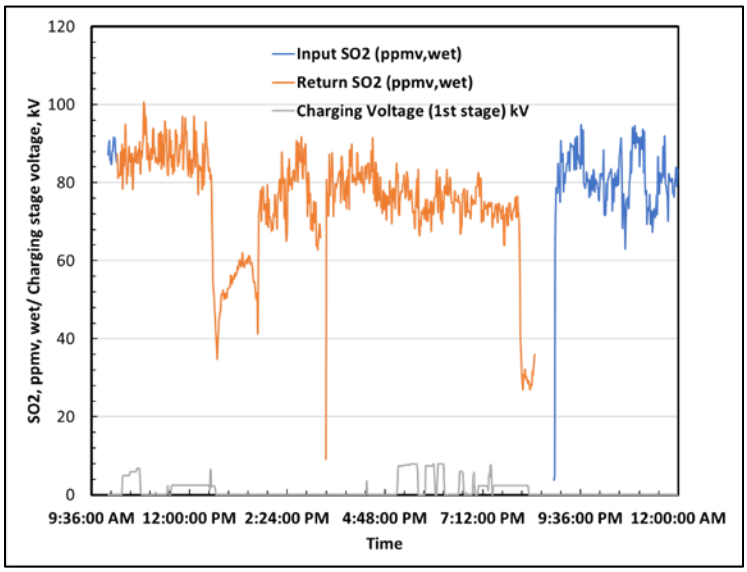

Figure 33: SO_2 concentrations measured at flue gas inlet and ESP outlet

C.2.4 InnoSepra sorbent filter testing for flue gas contaminant removal

Field tests were carried out using the test unit shown in Figure 34. The test unit contained 1,650 lbs. of sorbent. In addition to sample ports at the inlet and the outlet the unit contained several sample ports within the bed to monitor the progress of the sorption front. Prior to field testing at the Abbott Power Plant, quality control (QC) testing was carried out at the lab scale with the material used for field tests. The lab-scale test unit shown in Figure 34 was used for QC tests.

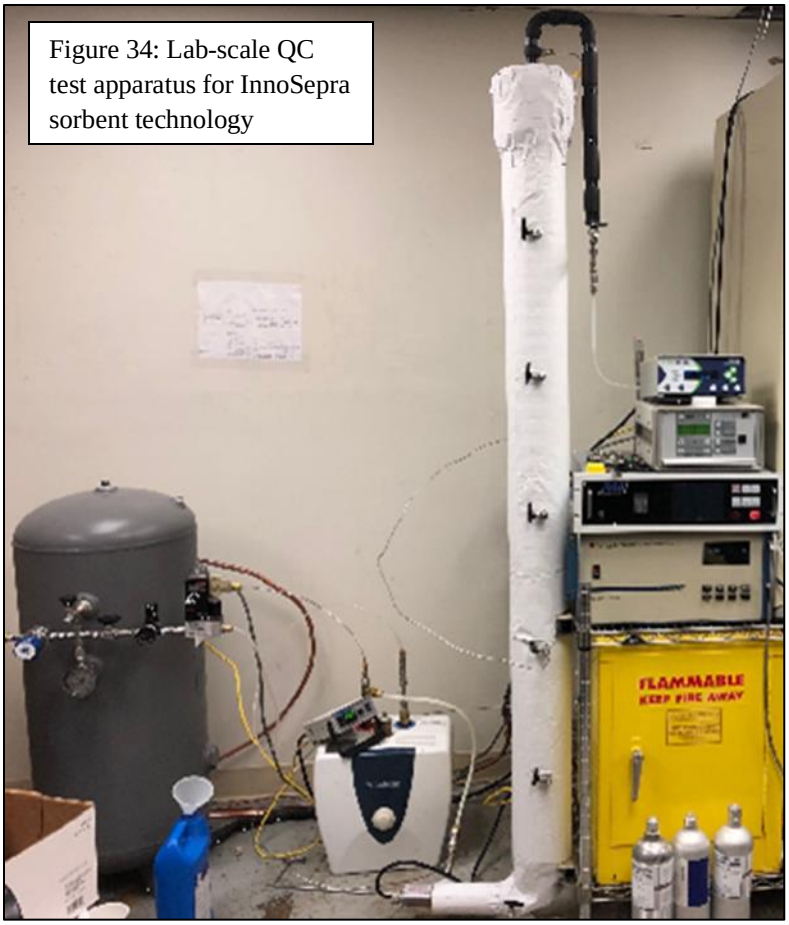

Figure 34: Lab-scale QC test apparatus for InnoSepra sorbent technology

For QC tests, the flow of compressed ambient air was controlled with a mass flow controller and bubbled through a temperature controlled hot water heater. The air exiting the hot water heater was saturated at its exit temperature and was further heated with a flow-through heater to the adsorption temperature. A small amount of SO_2 from a 5% SO_2 in nitrogen mixture was blended in this stream. The flow of the SO_2-N_2 mixture was controlled with a mass flow controller to obtain about 200-ppm SO_2 in the feed. The SO_2-air mixture entered the sorption bed with a 2" inner diameter. and a height of 6 ft. The sorption bed contains sample locations every foot. Gas samples streams from the feed sample port, sample ports at different locations in the bed, and the bed outlet were sent to a Thermo Model 43C SO_2 analyzer to monitor the progress of the adsorption front. The analyzer was calibrated with a 35-ppm SO_2 in nitrogen mixture and had a lower detection limit of 0.1-0.2 ppm. For these tests 1,904 g of sorbent was loaded in the bed and the SO_2-air mixture containing about 200 ppmv SO_2 was sent to the bed at a flow rate of about 24-slpm and a temperature of 104°F (40°C). The flow direction was from top to bottom based on the previous lab scale testing. This is also the flow direction for the field test unit. The QC lab-scale test results are shown in Figure 35. During about 240 hours of testing nearly complete SO_2 breakthrough was seen at location 1 (1-ft bed height) and partial breakthrough was seen at location 2. No SO_2 breakthrough was seen at any other location.

The equilibrium adsorption capacity is defined as:

Equilibrium capacity = Amount of SO_2 adsorbed until $t_{1/2}$ (50% breakthrough)/sorbent amount up to that location *100

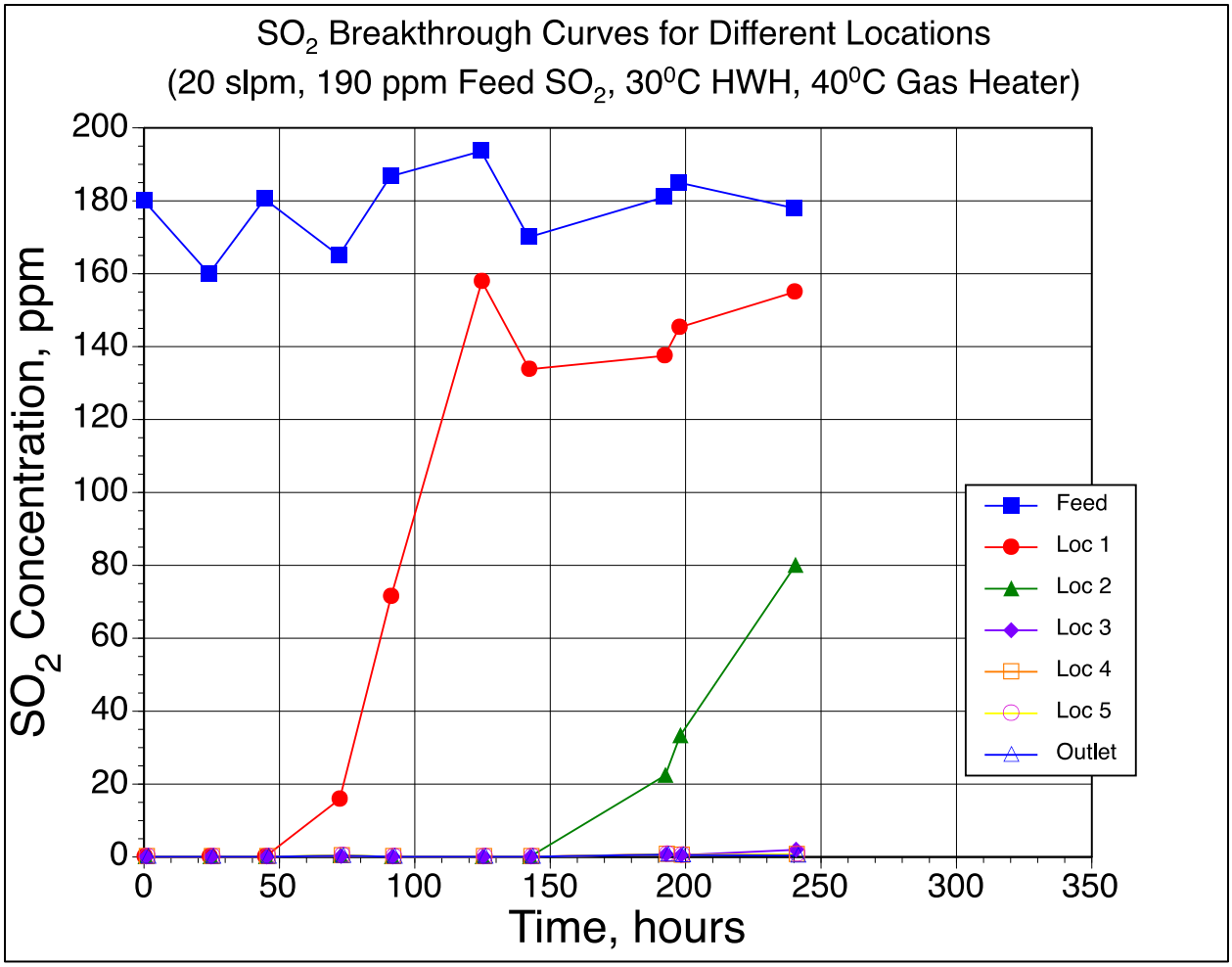

Figure 35: Lab-scale test breakthrough curve results for the InnoSepra sorbent material at 40°C feed temperature

Based on the adsorption capacity equation the equilibrium capacity for location 1 was 26 wt% and the equilibrium capacity for location 2 was 31 wt%. These capacities are based on SO_2 flowrates determined from the total air flow rate and the feed SO_2 concentration (based on analyzer calibration). An alternate way to determine the SO_2 flow rate is based on the SO_2 cylinder volume (1.04 ft^3), SO_2 concentration in the cylinder (5%), initial cylinder pressure (1,000 psig), and the final cylinder pressure (14.7 psia). Based on this method, the SO_2 capacity for location 1 was 33.5 wt% and the SO_2 capacity for location 2 was 40 wt%.

The InnoSepra pilot-scale tests were carried out for a period of over 160 hours at a flue gas flow rate of ~500 scfm. In addition to the feed, the SO_2 concentrations were monitored at sample port 5 (about 12" from the feed inlet) and sample port 4 (about 24" from the feed inlet). The average feed SO_2 concentration was about 130 ppmv (dry). Performance results are shown in Figure 36. No SO_2 breakthrough was seen at sample port 4 for the entire test period. Except for the initial increase at about 20 hours, 50% SO_2 breakthrough was not observed at sample port 5. Based on the sorbent mass up to sample port 5 the SO_2 capacity for the field test unit is very high, at least 29 wt%. This is closely in line with the sorbent capacity for the QC tests carried out in the lab.

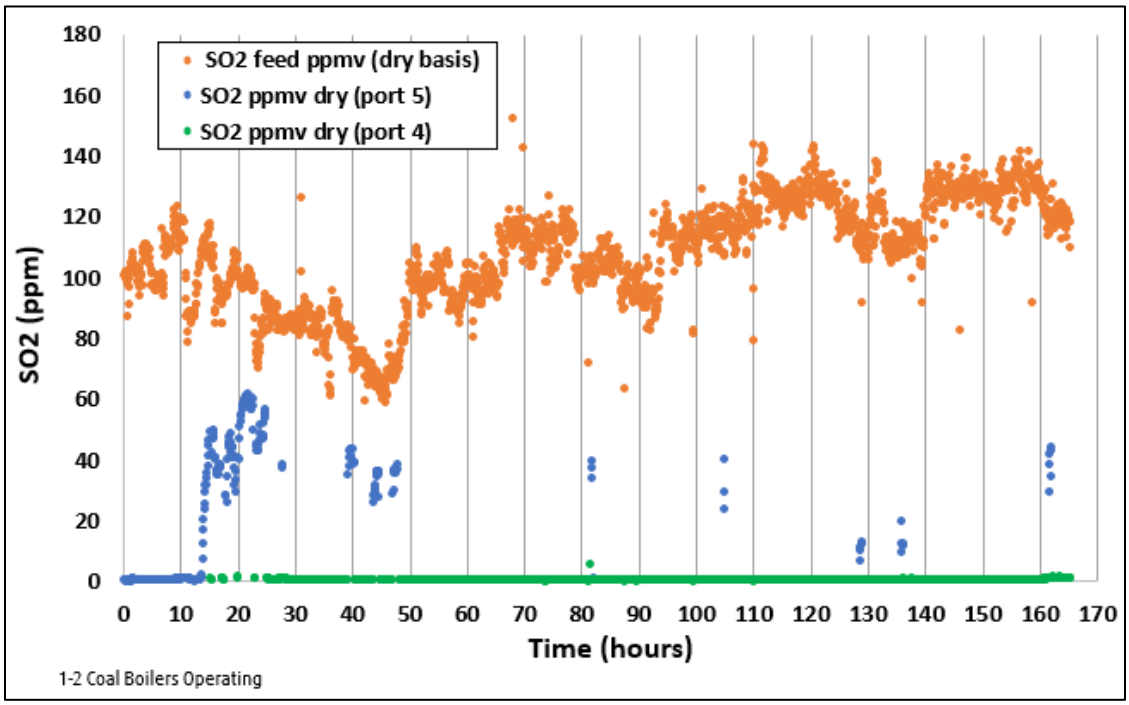

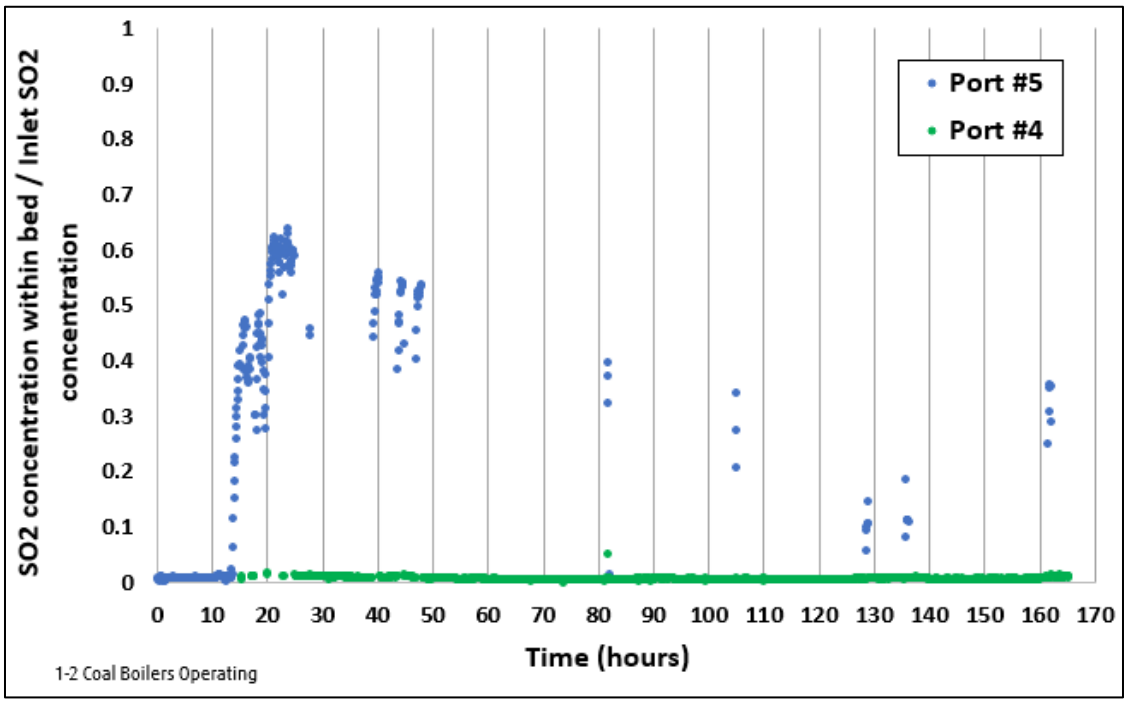

Figure 36: Pilot-scale SO_x removal performance for the InnoSepra sorbent technology

Figure 37 shows aerosol removal performance results for the InnoSepra filter for a series of pilot tests completed on two different days. These results show a typical particle removal profile for sorbent-based systems in which the filter has a reduced particle removal efficiency (30-70%) for a certain range of particle sizes (40-150 nm in this case) and higher efficiencies (up to +90%) for other sizes. The InnoSepra sorbent filter notably reduces aerosol concentrations. This particle removal performance, coupled with its demonstrated excellent SO_x removal ability and relatively low operating cost, make the InnoSepra sorbent filter a highly attractive option for flue gas purification and aerosol pretreatment for solvent-based PCC

systems. Table VII shows a summary of the numerical particle removal efficiency results from InnoSepra filter pilot testing.

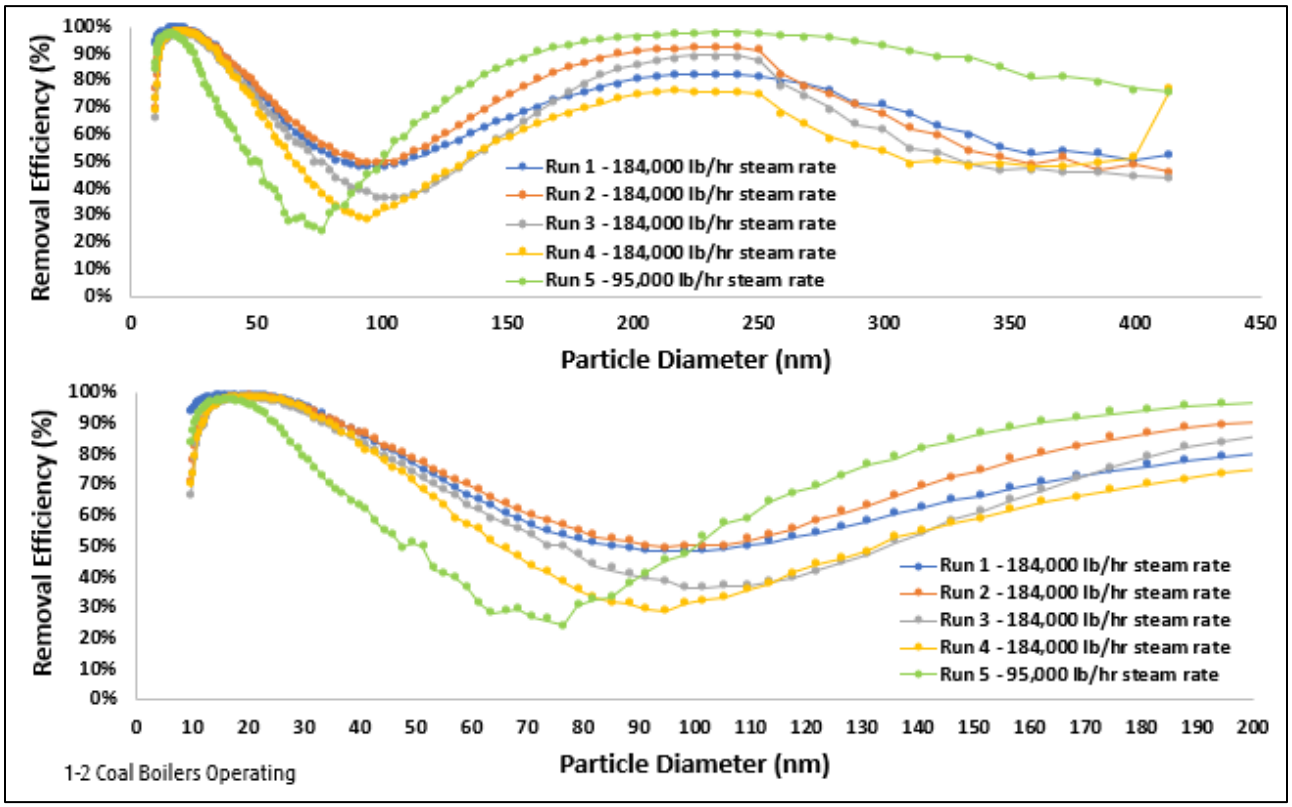

Figure 37: InnoSepra sorbent filter technology aerosol removal efficiency

Table VII: Summary of aerosol removal performance for InnoSepra sorbent filter by particle size

Particle Size Range (nm)	Average Aerosol Removal Efficiency (%)
9.8 to 30	94.33%
31.1 to 40	85.80%
41.4 to 51.4	79.49%
53.3 to 63.8	59.79%
66.1 to 82	46.94%
85.1 to 101.8	42.54%
105.5 to 126.3	50.40%
131 to 162.5	67.09%
168.5 to 201.7	81.87%
209.1 to 250.3	87.17%
Overall from 70 to 200 nm	58.15%

D. TECHNO-ECONOMIC ANALYSIS AND BENCHMARKING RESULTS

Based on cost estimates, a high-level techno-economic analysis (TEA) and benchmarking for the high-velocity water spray tower and ESP aerosol pretreatment systems has been completed that compares their economic attractiveness to that of a traditional baghouse particle removal system used in a coal-fired power plant. Table VIII shows cost factors and benefits for both technologies tested in this work. Since the InnoSepra filter system also provides SO_x removal, it is excluded from this analysis to provide a consistent comparison between technologies since the PCC technology reference used in this TEA is Shell's Cansolv

technology (DOE-NETL Case B12B, Ref. 11) and includes its own SO_x pretreatment. Power plant capital and operating cost components have been based on the Case B12B reference, which includes capital costs for a baghouse. Results from the TEA are shown in Table IX, Figure 38, and Figure 39. As mentioned, Case B12B and process cases 2-5 utilize the same solvent-based PCC technology (Shell Cansolv); however, cases 2-5 do not include the baghouse capital cost and parasitic energy penalty of a baghouse. For all cases in Table IX, it is assumed that the flue gas upstream of the PCC plant and any aerosol pretreatment system contains very high concentrations of aerosol particles ($>10^7$ particles/cm^3). Case 1 describes the scenario in which 4 times the normal solvent make-up rate is needed to operate the PCC plant due to a very high rate of aerosol-driven amine losses. While Case 2 is shown just for economic comparison, operating a PCC plant becomes logistically infeasible when extremely high amine solvent make-up rates are required to combat very high rates of aerosol-driven solvent losses. Thus, even if Case 2 were economically viable, the solvent delivery and operations challenges posed by unacceptably high solvent make-up rates would render Case 2 infeasible long-term at a continuously operating commercial PCC plant. For Case 3, even though modified absorber operating conditions can reduce aerosol-driven solvent losses, the effectiveness of modified operating conditions is only consistent if aerosol particle concentrations remain at a fixed level. Once aerosol concentrations increase to unacceptably high levels, even temporarily, changing absorber conditions cannot continue to compensate and solvent losses will eventually increase, leading to logistics challenges and high operating costs not included in Table IX. The PCC plant energy consumption shown for Case 3 will likely further increase depending on the range of absorber conditions needed to mitigate solvent losses. Hence, Case 3 is a temporary option and infeasible for long-term operation.

Table VIII: Cost factors and benefits for each flue gas aerosol pretreatment technology

Aerosol pre-treatment technology	Cost Factor 1 (High Impact)	Cost Factor 2 (Moderate Impact)	Cost Factor 3 (Low Impact)	Overall Benefits
RWE high-velocity water spray tower system	Capital cost for structural steel, spray injection vessel, piping, pump, spray nozzle, heat exchanger, and instrumentation	Operating costs (pumping energy, cooling media, process makeup costs, process condensate disposal cost, etc.)	Added PCC blower energy needed due to pressure drop across spray tower	Proven reduction in aerosol particle concentrations from pretreatment pilot test results and previous 0.5 MWe PCC pilot tests completed in Niederaussem, Germany
WUSTL ESP system	ESP capital cost, structural steel, instrumentation, and piping	Electricity consumption of ESP	Added PCC blower energy needed due to pressure drop across ESP	Proven reduction in aerosol particle concentrations from pretreatment pilot test results and lab testing completed at WUSTL

Baghouse costs of $48,784,000 (2011$) were evaluated based on DOE Case B12B (Ref. 12) for a 550 MWe (net) power plant; this power plant case was scaled up to the 650 MWe (net) size for the latest Case B12B with a single exponential scaling factor of 0.669 and a 3% escalation factor per year was applied to convert to 2018 cost year from 2011. With a 650 MWe power plant baghouse cost of $67,092 million, cases 4 & 5 offer a lower COE compared to DOE-NETL Case B12B with a baghouse. Hence, given these economic assumptions, the aerosol pretreatment solutions tested in this work offer superior economic benefits when integrated at power plants without baghouses compared to the scenario when those power plants invest in baghouses. In addition, compared to the proposed aerosol mitigation systems, construction and installation of a new baghouse at an existing power plant 1) requires significantly more footprint space, limiting its use

at power plants with space restrictions due to safety or operations concerns, 2) does not prevent aerosol generation downstream of the baghouse when the baghouse is built upstream of the flue gas desulfurization (FGD) unit or other systems, resulting in potentially higher aerosol concentrations in the flue gas entering a PCC plant, and 3) cannot counteract unexpected further increases in flue gas aerosol concentrations, especially for particles <200 nm, that lead to solvent losses since baghouse operating conditions remain constant. The proposed solutions offer flexibility to change operating parameters & design elements to increase aerosol removal efficiency for particular particle size ranges when needed. This analysis shows that the selected aerosol pretreatment systems evaluated in this project are the most economically attractive options to enable solvent-based PCC technology at power plants requiring aerosol pretreatment due to very high flue gas aerosol particle concentrations, especially if baghouse retrofit is physically infeasible or cost prohibitive.

Table IX: Techno-economic analysis comparing cost (2018$) and performance of supercritical power plants integrated with PCC with and without flue gas aerosol pretreatment. PP = Supercritical PC 650 MWe (net) power plant with high flue gas aerosol concentrations leading to high amine losses for an integrated PCC plant when no aerosol pretreatment is used.

Scenario	Case 1: DOE-NETL Case B12B: PP w/ 90% CO_2 capture	Case 2: PP w/ 90% CO_2 capture; 4X solvent make-up needed to offset high solvent losses	Case 3: PP w/ 90% CO_2 capture; varying absorber conditions to reduce solvent losses	Case 4: PP w/ 90% CO_2 capture; High-velocity water spray aerosol pretreatment	Case 5: PP w/ 90% CO_2 capture; Advanced ESP aerosol pretreatment
Baghouse	Yes, has baghouse	No baghouse	No baghouse	No baghouse	No baghouse
Power Plant Gross Power (MWe)	770.0	767.3	770.8	780.5	770.5
Auxiliary Power (MWe)	120.0	117.7	121.1	130.5	120.8
Power Plant Net Power (MWe)	650	650	650	650	650
Net Power Plant HHV Efficiency (%)	31.51%	31.59%	30.63%	31.10%	31.50%
Added CAPEX w/ aerosol pretreatment ($)	N/A	N/A	N/A	$3,261,720	$6,417,014
Added energy consumption w/ aerosol pretreatment (MW)	N/A	N/A	N/A	11	2.64
Total Overnight Cost ($)	$3,099,688,639	$3,026,997,735	$3,081,915,999	$3,055,857,753	$3,034,771,810
PCC plant specific energy consumption (MJ/kg CO_2)	2.43	2.43	3.01	2.43	2.43

Cost of electricity w/o T&S ($/MWh)	**$106.51**	**$110.96**	**$107.54**	**$106.38**	**$105.54**
Cost of electricity w/ T&S* ($/MWh)	**$115.41**	**$119.84**	**$116.70**	**$115.40**	**$114.45**
Cost of CO_2 captured w/ T&S* ($/tonne)	**$57.05**	**$62.15**	**$56.85**	**$56.29**	**$55.89**
***T&S cost = $9.95/tonne CO_2**					

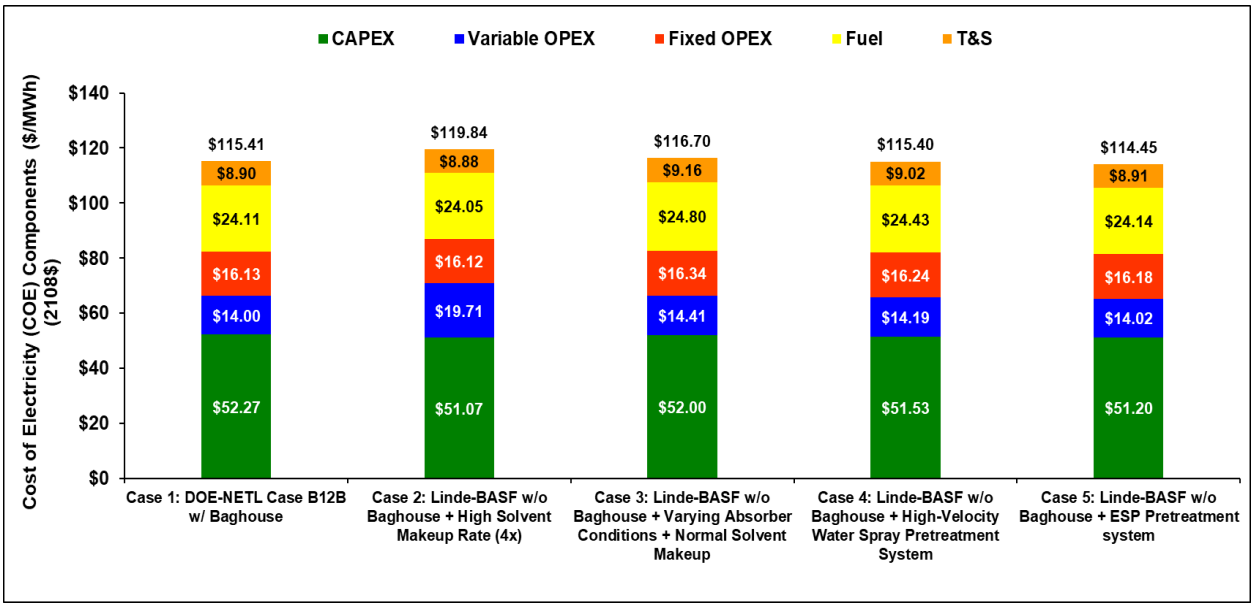

Figure 38: Cost of electricity components ($/MWh) for each pretreatment option evaluated (Cases 4 & 5) compared to DOE-NETL Case B12B w/ baghouse and other process scenarios

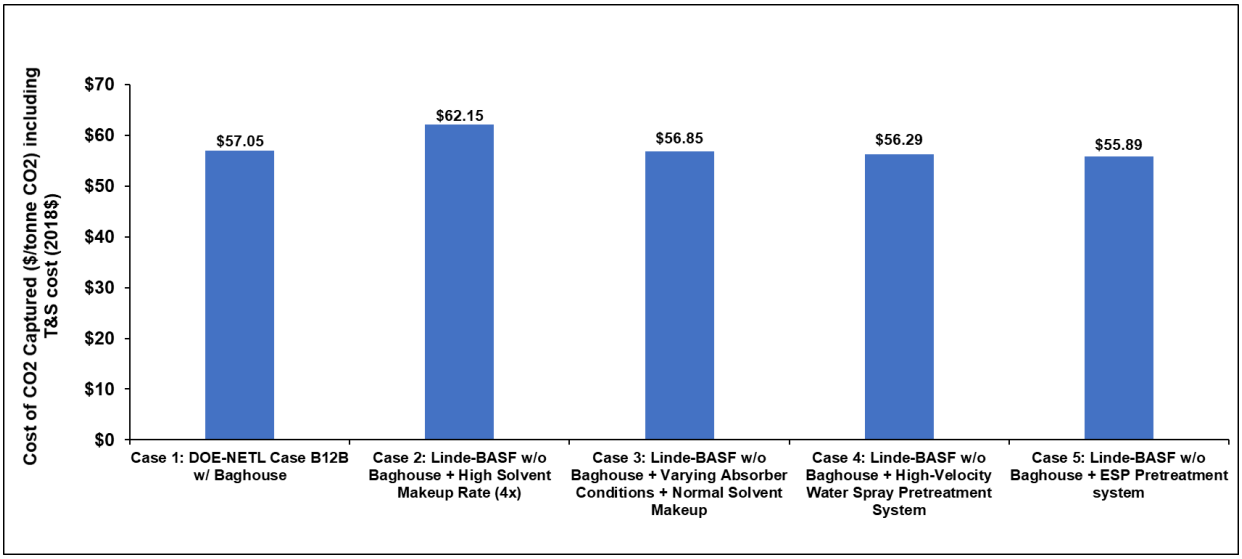

Figure 39: Cost of CO_2 captured ($/tonne CO_2) for each pretreatment option evaluated (Cases 4 & 5) compared to DOE-NETL Case B12B w/ baghouse and other process scenarios

E. RECOMMENDATIONS FOR FUTURE WORK AND NEXT STEPS

During the pilot test campaign, the operations team discovered several design features that would be helpful for future scale-up and implementation in a large demonstration with a CO_2 capture plant. The following are features to implement for all aerosol pretreatment systems:

1) For future pilot studies requiring aerosol measurements, piping layout should be designed with a sufficient length of straight pipe upstream of the sampling probe to achieve isokinetic sampling and uniform particle distribution in the pipe. Flue gas supply and return pipe segments were designed with sufficient straight pipe length needed for accurate aerosol measurements; however, the inlets to each individual process unit (spray tower, ESP, and sorbent filter) had natural bends required for optimal flow paths. In a full-scale commercial system, such pipe bends would not be necessary as the process skid can be optimally designed for one technology. Combining three technologies into one process skid with two main supply and return gas headers required piping bends to limit use of excessive piping that would have otherwise greatly increased the capital cost of the system.

2) Gas piping and components should be insulated, and heat traced (if required) to prevent condensation of flue gas moisture and aerosol loss. Additionally, low point water condensate drains needed to be added to the inlet of each pilot sub-system instead of one main drain. A water condensate drain installed right at the inlet to the sorbent filter and ESP would have helped remove water and prevent water-related flow obstruction. The process piping to and from the pilot skid was installed without insulation to save installation costs as the power plant flue gas supply was superheated at the inlet (up to 40-50°F superheat) and estimations of heat loss during the design phase showed minimal condensation potential. The issue observed during operations was that the flue gas supply temperature changed dramatically through each day and between operating days. This inconsistency led to excessive condensation during certain periods and resulted in aerosol removal performance differences. To help manage unexpected changes in flue gas temperatures, process piping should be well insulated, and heat traced as needed in especially cold geographies during winter months.

3) To save start-up and commissioning time, aerosol measurement equipment should be thoroughly checked for leaks before installation and designed with stainless steel components to ensure long-term reliable use. Tubing should also be insulated and fully heat traced along the entire length of sample probe. The pilot system included insulation for the entire length of each sample probe but only 60-70% of each sample line was effectively heat traced due to equipment limitations in the commissioning phase. Incomplete heat tracing and insulation can lead to water condensation and aerosol removal, which can lead to inconsistent performance results.

Future recommendations for the ESP system in particular:

1) Alternatives to polyether ether ketone (PEEK) should be considered for ESP electrical insulation inside the charging and collection stages, as PEEK is susceptible to thermal damage and electrical arcing in the presence of water (vapor and condensate) from the saturated flue gas. Lab test results without the presence of water showed excellent PEEK material performance, but pilot tests have shown that water in the flue gas is not compatible with PEEK as an insulation material. New materials of construction must be identified and evaluated for the next demonstration testing on real coal-fired flue gas.

2) Design improvements to the ESP should be made to direct any water condensation away from high-voltage internal components during cold startup.

3) ESP collection efficiency can be further improved with higher operating voltage (charging stage). This can be achieved with improved high-voltage insulation and design with greater resistance to water from the flue gas and increased spacing between high voltage components and the system structure connected to the ground.

4) Incorporation of soft X-ray sources to improve the collection efficiency of nano-scale aerosol particles requires custom components to withstand conditions of high temperature, high humidity, and SO_x content.

5) Higher collection efficiency can be achieved by reversing the polarity of the ESP (Ref. 13). This requires alternative power supplies.

6) Since particulate concentrations in flue gas were found to be highly variable even within short time frames, the accuracy of the collection efficiency measurement can be improved with duplicate instruments

to simultaneously measure filter inlet and outlet. To minimize pilot system cost, only one set of aerosol measurement equipment was used during the flue gas test campaign and this was used separately for flue gas supply and return measurements at different points in time under the same operating conditions and pretreatment system operating modes.
7) Spacing of the ESP collection plates should be increased to reduce the likelihood of electrical arcing and buildup of flue gas debris forming bridges between the plates. Excessive buildup of debris of the collection plates leads to shorting and increases the time required for routine maintenance cleaning of the plates. Elimination of this debris and electrical arcing potential will enable a higher operating collection stage voltage and therefore much higher aerosol removal efficiencies at commercial scales.
8) An automated method for cleaning the ESP collection plates should be developed for the next demonstration scale.
(9) The collection efficiencies measured at the Abbott Power Plant were lower than the efficiencies measured at ACERF using aerosol-laced air due to the following reasons:

- The non-insulated piping of the flue gas leading to the ESP resulted in condensation of water given the freezing temperatures during the months of January – March at the site.
- The increased moisture content in the flue gas affects the insulating functionality of PEEK (reduces electrical resistivity) and results in arcing at higher voltages
- The reduced electrical resistivity of the charging station insulating material limited the voltage at which the ESP can be operated leading to reduced collection efficiencies.

F. CONCLUSIONS

Depending on the design component used, pilot tests have shown that the RWE high-velocity water spray tower technology can achieve 85-90% aerosol removal efficiencies for particles within the 70-200 nm size range of interest for mitigating aerosol-driven amine losses from solvent-based PCC plants. The WUSTL ESP technology demonstrated removal efficiencies of up to 80% at the highest voltage tested, but the ESP was limited by the actual voltage that could be applied due to electrical arcing as a result of inadequate material insulation for the charging stage. ESP design and material analysis work will be completed as the next step following pilot tests to enable higher operating ESP voltages to achieve greater particle removal efficiencies for sustained periods of time. The InnoSepra sorbent filter was able to achieve >99% SO_2 removal from the flue gas and aerosol removal efficiencies from 30-90% within the 70-200 nm size range. These aerosol removal efficiencies are relative to supply flue gas aerosol concentrations of up to 4E+07 particles/cm^3 and flue gas flowrates between 500 and 1000 scfm. Based on a preliminary techno-economic analysis at commercial-scale, the high-velocity spray tower and ESP systems tested in this work provide economically attractive flue gas aerosol pretreatment for a solvent-based PCC plant integrated with a coal-fired power plant in comparison to baghouse pretreatment while also providing operational flexibility, a smaller footprint, and solvent loss optimization that can be tailored to the specific capture process.

G. REFERENCES

1) P. Moser, G. Weichers, K. Stahl, T. Stoffregen, G. Vorberg, G. Lozano; *Solid Particles as Nuclei for Aerosol Formation and Cause of Emissions – Results from the Post-Combustion Capture Pilot Plant at Niederaussem*, GHGT-13, Energy Procedia 2017; 114: Pages 1000-1016.

2) D. Bostick, K. Krishnamurthy; *Final Testing Report to NCCC*, DOE-NETL Contract No. DE-FE0007453, Murray Hill, NJ, 2017.

3) Y. Wang, Z. Li, P. Biswas; *Aerosol Measurements in Coal Combustor Exhaust Gas on 1.5 MWe Advanced Aqueous Amine-Based PCC Pilot Plant in Wilsonville, AL*, Washington University in St. Louis, August 8, 2016.

4) Y. Wang, Z. Li, P. Biswas; *Aerosol Measurements in Coal Combustor Exhaust Gas at Abbott Power Plant, IL*, Washington University in St. Louis, February 22, 2016.

5) G. Lombardo, B. Fostas, M. Shah, A. Morken, O. Hvidsten, J. Mertens, E. Hamborg; *Results from Aerosol Measurement in Amine Plant Treating Gas Turbine and Residue Fluidized Catalytic Cracker Flue Gases at the CO_2 Technology Centre Mongstad*, GHGT-13, Energy Procedia 2017; 114: Pages 1210-1230.

6) P. Moser, G. Vorberg, T. Stoffregen, et. A; *The wet electrostatic precipitator as a cause of mist formation – Results from the amine-based post-combustion capture pilot plant at Niederaussem*. International Journal of Greenhouse Gas Control, 41 (2015) 229–238.

7) C. Saha, J. Irvin; *Linde Aerosol Characterization Tests Conducted at the National Carbon Capture Center*, Energy and Environment, Southern Research, January 22, 2016.

8) C. Saha, L. Berry; *Linde Aerosol Characterization Tests Conducted at the National Carbon Capture Center*, Energy and Environment, Southern Research, February 2, 2017.

9) S. Fulk, M. Beaudry, G. Rochelle; *Amine Aerosol Characterization by Phase Doppler Interferometry*, GHGT-13, Energy Procedia 2017; 114: Pages 939-951.

10) S. Jovanovic, K. Krishnamurthy, Y. Lu, S. Rigby, T. Stoffregen; *Phase 1 Technology Gap Analysis, DOE-NETL Contract No. DE-FE0026588*, Murray Hill, NJ, March 31, 2016.

11) DOE-NETL. *Cost and Performance Baseline for Fossil Energy Plants, Volume 1: Bituminous Coal and Natural Gas to Electricity*, September 24, 2019.

12) DOE-NETL Office of Fossil Energy. *Cost and Performance Baseline for Fossil Energy Plants, Volume 1a: Bituminous Coal (PC) and Natural Gas to Electricity*, Revision 3, July 6, 2015.

13) P. Kulkarni, N. Namiki, Y. Otani, and P. Biswas, *Charging of particles in unipolar coronas irradiated by in-situ soft X-rays: enhancement of capture efficiency of ultrafine particles*, Aerosol Science, vol. 33, pp. 279–1296, 2002